Universität Bremen

The University of Queensland
AUSTRALIA

Marine Biology, M.Sc.

MASTER'S THESIS

Physiological adaptations of mesophotic corals across a depth gradient

–

Leptoseris spp. & *Pachyseris speciosa*
(Scleractinia: Agariciidae)

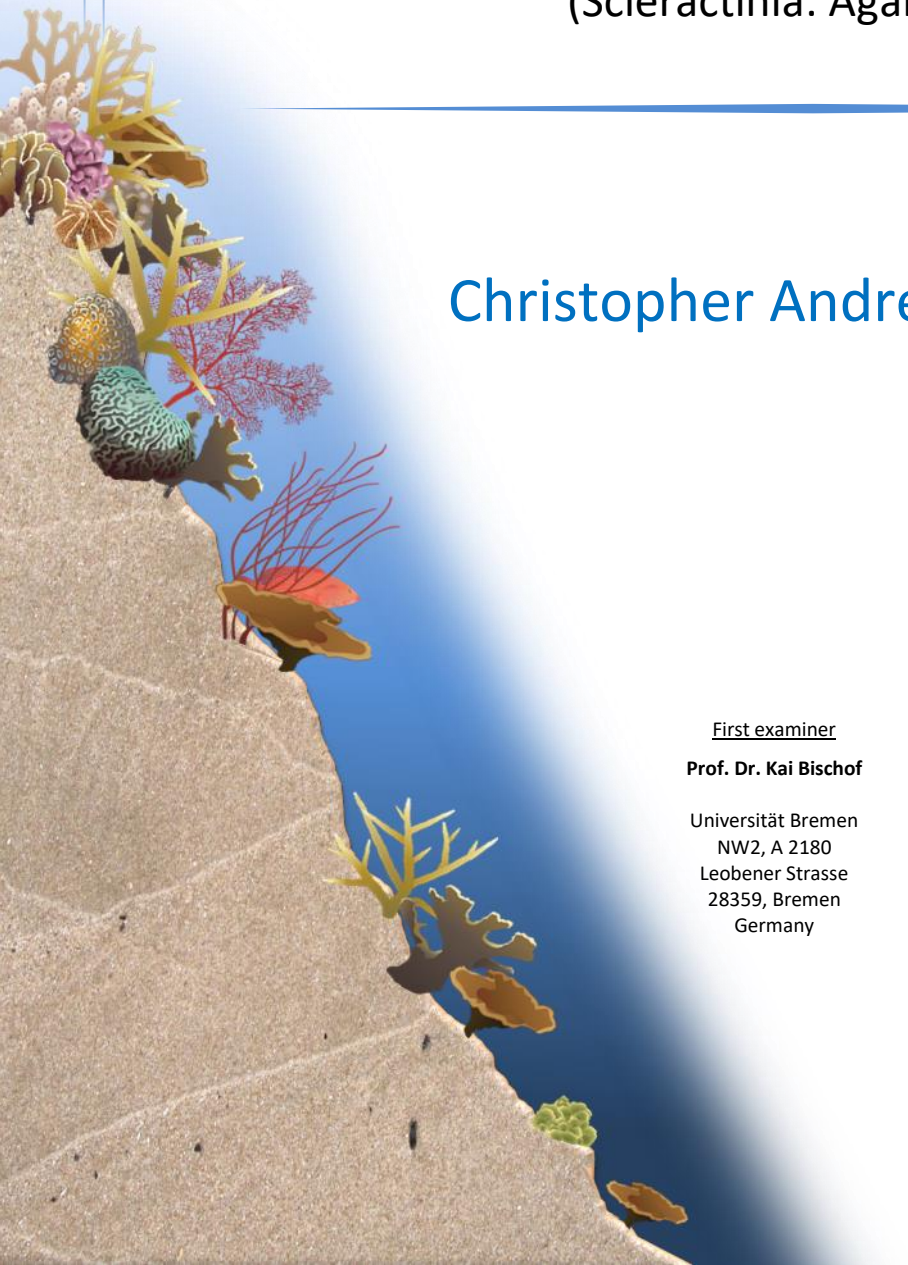

Christopher Andreas Nowak

First examiner
Prof. Dr. Kai Bischof
Universität Bremen
NW2, A 2180
Leobener Strasse
28359, Bremen
Germany

Second examiner
Assoc. Prof. Dr. Sophie Dove
Coral Reef Ecosystems Lab
The University of Queensland
Gehrmann Building
4072, St Lucia, QLD
Australia

Daily supervisor
Norbert Englebert
Coral Reef Ecosystems Lab
The University of Queensland
Gehrmann Building
4072, St Lucia, QLD
Australia

In memory of my grandparents.

List of contents

List of figures

List of equations

List of tables

Abbreviations

Abbreviation	Description
ANOVA	Analysis of Variance
Chl *a*	Chlorophyll *a*
Chl c_2	Chlorophyll c_2
Ddx	Diadinoxanthin
DRRH	Deep Reef Refugia Hypothesis
Dtx	Diatoxanthin
Fuco	Fucoxanthin
HPLC	High-Performance Liquid Chromatography
LH	Light-harvesting
MCE	Mesophotic Coral Ecosystem
N/A	Not Available
PC	Principal Component
PCA	Principal Component Analysis
Per	Peridinin
PP	Photoprotective
ROV	Remote Operated Vehicle
SCUBA	Self-Contained Underwater Breathing Apparatus
SE	Standard Error
ß-caro	*ß*-carotene

Keywords

Leptoseris spp., *Pachyseris speciosa*, *Symbiodinium*, photo-adaptation, mesophotic coral ecosystem

Abstract

Climate-induced stressors, such as intensifying storms, temperature anomalies, or bleaching events may less affect corals thriving in the mesophotic zone (30 - 150 m water depth) compared to corals in shallower areas. Hence, the scientific interest increased during the last years, since mesophotic corals may act as source of recruitment for affected shallower reefs. However, even basic mechanisms of these zooxanthellate corals still represent pronounced scientific gaps. Accordingly, knowledge of the photo-physiology and adaptations towards decreasing light availability with increasing water depth of the dominating and cosmopolitan coral genera *Leptoseris* and *Pachyseris* is scarce. Within this study, physiological adaptations of *Leptoseris scabra*, *Leptoseris glabra*, *Leptoseris hawaiiensis* and *Pachyseris speciosa* across a large water depth range (10 – 80 m) at the Osprey Reef (Coral Sea) were investigated. Via an integrated approach, the synergy of distinct photo-biological strategies was evaluated (v). Accordingly, physiological adjustments of the coral host (skeletal density, tissue thickness and lipid concentration) (ii), *Symbiodinium* adaptations (cell size, cell density and mitotic index) (iii), as well as the composition of light-harvesting and photo-protective pigments (iv) were distinguished. The analyses revealed that corals of the genera *Leptoseris* and *Pachyseris* follow different strategies to adapt towards decreasing light intensities across a large depth gradient (i). Specimen of *Pachyseris speciosa* showed morphological adaptations across an 80 m depth gradient in form of significantly decreasing tissue thickness (43%) and a strong negative trend of the *Symbiodinium* density (41%). This, presumably was coupled with a rearrangement of the *Symbiodinium* cells towards mono-layers to reduce self-shading. In contrast, within corals of the genus *Leptoseris*, morphologically only a significant decrease of the *Symbiodinium* size (22%) was observable with increasing depth. Overall, both genera had in common that a decrease of photoprotective pigments, rather than an increase of light-harvesting pigments was observable.

In summary, for the coral genera *Leptoseris* and *Pachyseris*, predominantly the synergy of morphological adaptations of the coral host, morphological adaptations of the harboured symbionts, as well as decreasing photoprotective pigment concentrations, seem to be the key for a successful colonisation of a large depth gradient.

Zusammenfassung

Zerstörerische Klimaeinflüsse, wie zum Beispiel tropische Stürme, Korallenbleichen oder erhöhte Temperaturen des Oberflächenwassers, beeinflussen Korallen der mesophotischen Zone (30 – 150 m Wassertiefe) nur verminderter. Aus diesem Grund wächst das wissenschaftliche Interesse an diesen mesophotischen Korallen immer weiter, da vermutet wird, dass Sie zur Restaurierung flacherer Riffe beitragen könnten. Jedoch werfen selbst grundlegende Mechanismen, wie etwa die Fotophysiologie, dieser mesophotischer Korallen noch immer Fragen auf. Durch Ihre Endosymbiose mit Zooxanthellen, sind sie auf das Sonnenlicht angewiesen und müssen deshalb über ausgeprägte Adaptationsmechanismen verfügen, welche das Leben entlang eines großen Tiefengradienten überhaupt erst ermöglichen. Dabei ist selbst von den dominierenden mesophotischen Korallengattungen *Leptoseris* und *Pachyseris* noch immer wenig bekannt. Aus diesem Grund wurden Individuen der Arten *Leptoseris scabra, Leptoseris glabra, Leptoseris hawaiiensis* und *Pachyseris speciosa* untersucht, welche aus 10 – 80 m Wassertiefe vom Osprey Reef (Korallenmeer) stammten. Es wurden die physiologischen Adaptation der Korallen (Skelettdichte, Gewebedicke und Lipid Konzentration) (ii), die Adaptionen der Zooxanthellen (Zellendurchmesser, Zellendichte und mitotischer Index) (iii) und die Konzentrationsänderungen von lichtsammelnden, sowie abschattenden Pigmenten gemessen (iv), und in Relation zueinander betrachtet (v). Die Analysen haben gezeigt, dass Korallen der Gattungen *Leptoseris* und *Pachyseris* unterschiedliche Strategien verfolgen, um sich der abnehmenden Lichtintensität innerhalb eines Tiefengradienten anzupassen (i). Individuen der Art *Pachyseris speciosa* zeigten morphologische Adaptation zwischen 10 und 80 m Wassertiefe in Form von signifikant verminderter Gewebedicke (43%), sowie stark abnehmenden Trends der Zooxanthellen Zellendichte (41%). Dies war höchstwahrscheinlich mit einer Umverteilung der Zooxanthellen innerhalb des Gewebes von mehreren Schichten zu einfachen Schichten gekoppelt. Dem entgegen zeigten Arten der Gattung *Leptoseris* signifikante Veränderungen durch Verringerung des Zooxanthellendurchmessers (22%) entlang des Tiefengradienten. Beide Gattungen hingegen, zeigten signifikante Reduzierungen der abschattenden Pigmente, nicht aber signifikante anstiege der lichtsammelnden Pigmente.

Damit lässt sich zusammenfassen, dass für die dominanten mesophotischen Korallen Gattungen *Leptoseris* und *Pachyseris* vor allem das Zusammenwirken von morphologischen Adaptationen der Koralle und der endosymbiontischen Zooxanthellen, sowie eine Reduzierung von abschattenden Pigmente der Schlüssel für eine Erfolgreiche Kolonisierung entlang eines großen Tiefengradienten sind.

1 Introduction

1.1 Mesophotic coral reefs

One of the most productive and biologically diverse ecosystems of our planet are coral reefs (Connell, 1978). They provide habitat and shelter for numerous animals, especially during their early life stages (Nagelkerken *et al.*, 2000; Adams *et al.*, 2006). In this way, they form the basis of the fishing industry of several nations (Graham *et al.*, 2007; Hoegh-Guldberg *et al.*, 2007; Pratchett *et al.*, 2008). Furthermore, reefs protect islands and coastlines from wave stress (Spencer, 1985; Sunamura, 1992), which becomes EVEN more important in times of intensifying storms. Anthropogenic and climate induced influences, such as uncontrolled tourism, destructive fishing methods, coral diseases, ocean acidification, sea surface temperature anomalies as well as bleaching events, resulted in major coral cover loss over the last decades (Brown, 1990; Hoegh-Guldberg, 1999; Moberg and Folke, 1999; Wellington *et al.*, 2001; Hughes *et al.*, 2003; Hoegh-Guldberg *et al.*, 2007; Baker *et al.*, 2008; Palumbi *et al.*, 2014). Although some disturbances may also affect coral reefs over the entire depth range (e.g. sedimentation, nutrient enrichment and influx of toxins) (Bongaerts *et al.*, 2010a), it has been shown that corals from deeper waters (>30 m) are less affected by the previously mentioned stressors (Liddell and Ohlhorst, 1988; Glynn, 1996; Bongaerts *et al.*, 2010a). Therefore, a rising interest in corals with phototrophic obligate symbionts (dinoflagellates of the genus *Symbiodinium*) from greater depths emerged. However, primarily traditional SCUBA diving limitations (maximal diving depth = 40 m) constrained the research in the deep. Therefore, these ecosystems still represent a huge knowledge gap in reef science (Bongaerts *et al.*, 2010a; Hinderstein *et al.*, 2010). Recent technological developments (closed-circuit mixed-gas diving, remote operated vehicles (ROVs), manned submersibles, etc.) simplified and improved the accessibility of these remote areas. In this way, it became possible to verify that these mesophotic coral ecosystems (MCEs) thrive in tropical and subtropical regions and can be encountered from 30 m down to depths at which the irradiance is too low to sustain the growth of zooxanthellate corals, which can be 150 m and beyond (Bongaerts *et al.*, 2010a; Hinderstein *et al.*, 2010; Kahng *et al.*, 2010; Englebert *et al.*, 2014). These great depths of MCEs led to the 'deep reef refugia' hypothesis (DRRH), postulated by Glynn (1996), which gained more and more popularity in the literature (Hughes and Tanner, 2000; Feingold, 2001; Glynn *et al.*, 2001; West and Salm, 2003; Riegl and Piller, 2003; Armstrong *et al.*, 2006; Venn *et al.*, 2009; Bongaerts *et al.*, 2010a; Hinderstein *et al.*, 2010; Bongaerts *et al.*, 2011; van Oppen *et al.*, 2011; Kahng *et al.*, 2014; Bongaerts *et al.*, 2015; Ziegler *et al.*, 2015). It assumes that MCEs function as refugia during periods of stress and subsequently function as source of propagules for recovering affected shallow reef habitats. However, Bongaerts *et al.* (2010a) and Slattery *et al.* (2011) note that (genetic)

connectivity over a very large depth range may be limited; but connectivity over smaller depth spans, such as between shallow reefs and upper mesophotic habitats, as well as upper mesophotic and lower mesophotic reefs, might be possible.

1.2 Coral ecophysiology in deep reefs

The viability of zooxanthellate corals in low-light conditions highly depends on their adaptability, which can take place in multiple ways and is highly interrelated (Falkowski and Dubinsky, 1981; Dustan, 1982; Porter *et al.*, 1984; Kirk, 1994; Anthony and Hoegh-Guldberg, 2003; Dove *et al.*, 2008; Frade *et al.*, 2008a, 2008b; Dubinsky and Stambler, 2009; Kahng *et al.*, 2010; Cooper *et al.*, 2011; Bongaerts *et al.*, 2015; Ziegler *et al.*, 2015). Thereby, adaptations may be regulated by the hosting coral or by the inhabiting symbiont (Ziegler *et al.*, 2015). In general, appropriate strategies are represented by the reduction of metabolic requirements (Kahng *et al.*, 2010), photo-acclimatization (Porter *et al.*, 1984) or morphological adaptations. As such, coral colonies show more filigree, broader and thinner growth habit with increasing depth to reduce self-shading and therewith maximizing the light harvesting potential (Kühlmann, 1983; Anthony and Hoegh-Guldberg, 2003; Enríquez *et al.*, 2005; Nir *et al.*, 2011; Kahng *et al.*, 2012; Englebert *et al.*, 2014). Furthermore, also changes on micro-skeletal level are possible to enhance the light-capturing capacity, as shown for *Leptoseris* spp. (Kahng *et al.*, 2012). In contrast to their relatives from shallow-waters, *Leptoseris* spp. colonies from lower mesophotic regions (70 – 130 m) feature perfectly parallel septo-costae. Kahng *et al.* (2012) showed that this skeletal design increases the path length of light within the tissue, resulting in much greater light-harvesting with less pigment per unit area. Although the increase of symbiont volume, coupled with increasing pigment concentrations, or the rise of symbiont density is a common adaptation (Venn *et al.*, 2006), it has been shown that with increasing depth, the *Symbiodinium* concentration decreases of several scleractinia (Kahng *et al.*, 2012). This probably occurs to minimize self-shading of the symbionts due to a shift from multi-layer symbiont arrangements in shallow-waters to mono-layers in the deep (Dustan, 1979; Schlichter *et al.*, 1985, 1986; Fitt *et al.*, 2000). Therewith, also the tissue biomass per unit surface area over depth decreases (Dustan, 1979; Anthony and Hoegh-Guldberg, 2003). Besides these adaptations related to the coral host, also the inhabiting symbiont buries adjustments to improve the survival across decreasing light levels. Hence, the harboured symbiont genotype may change across decreasing levels of irradiance towards more acclimatized types of a certain light regime (Iglesias-Prieto *et al.*, 2004; LaJeunesse *et al.*, 2005; Frade *et al.*, 2007, 2008b, 2008a; Bongaerts *et al.*, 2010b). In addition to that, also the colour morph of a certain symbiont may influences the pigment concentrations and consequently the photo-adaptability (Dove *et al.*, 2006, 2008). Within the *Symbiodinium* cells, low-light situations typically lead to an enrichment of the light-harvesting (LH) pigment chlorophyll *a* (Chl *a*) (Falkowski and

Dubinsky, 1981; Kirk, 1994; Dubinsky and Stambler, 2009; Kahng *et al.*, 2012) coupled with an increase of accessory pigments, such as chlorophyll c_2 (Chl c_2), fucoxanthin (Fuco) or the dinoflagellate-specific pigment peridinin (Per) (Iglesias-Prieto and Trench, 1994; Dove *et al.*, 2006). Thereby, the concentration of *ß*-carotene (*ß*-caro), as well as the amount of the xanthophylls diadinoxanthin (Ddx) and diatoxanthin (Dtx) commonly decreases, since they represent photoprotective (PP) pigments (Jeffrey and Haxo, 1968; Falkowski and Dubinsky, 1981; Kirk, 1994; Brown *et al.*, 1999; Dubinsky and Stambler, 2009; Kahng *et al.*, 2012). However, in extreme situations (> 100 m depth) the excessive increase of light-harvesting pigments may results in self-shading (Fricke *et al.*, 1987; Falkowski *et al.*, 1990), making this strategy ineffective for zooxanthellate mesophotic corals in greater depths (Enríquez *et al.*, 2005). This demonstrates how little is known about the photic-system and the recipe for success of mesophotic corals across a large depth gradient.

1.3 Gaps of knowledge

To date, most studies of MCEs have been focusing on taxonomic composition, depth range and habitat preferences of species in the Caribbean and the Indo-Pacific (e.g. Liddell and Ohlhorst, 1988; Glynn, 1996; Bongaerts *et al.*, 2010a; Hinderstein *et al.*, 2010; Kahng *et al.*, 2010; Holstein, 2013; Bongaerts *et al.*, 2015). Furthermore, a few studies in the Red Sea have been carried out (e.g. Fricke *et al.*, 1987; Nir *et al.*, 2011; Ziegler *et al.*, 2015). In general, these studies show that two of the highly dominating mesophotic coral genera in the Indo-Pacific are represented by *Leptoseris* and *Pachyseris*, in particular *Leptoseris hawaiiensis* Vaughan, 1907 and *Pachyseris speciosa* (Dana, 1846) (Vareschi and Fricke, 1986; Kahng *et al.*, 2010; Bongaerts *et al.*, 2011; Kahng *et al.*, 2014; Ziegler *et al.*, 2015).

Both, *L. hawaiiensis* and *P. speciosa*, can be classified as zooxanthellate depth-generalist corals due to their flexibility to thrive under a great variety of environmental conditions (Veron, 2000). In this way, they are able to span shallow and mesophotic depths, with the deepest recorded *L. hawaiiensis* colony at 165 m (Maragos and Jokiel, 1986) and the deepest recorded *P. speciosa* individuals at approximately 120 m depth (Abbey *et al.*, 2013). Either species can occur partly encrusting, but typically forms plate-like colonies, which can be erected to create vase-like structures (Veron, 2000). *L. hawaiiensis* can be distinguished by its protuberant corallites and equally sized septo-costae with even appearance, while *P. speciosa* is primarily characterized by its predominant concentric ridges parallel to the edge of the colony (Veron, 1986).

Although the coral genera *Leptoseris* and *Pachyseris* dominate a vast number of mesophotic reefs in the Indo-Pacific, still little is known about their recipe for success. Slow growth and metabolism is a common strategy for the survival in an energy-limited environment (Baker *et al.*, 2015). However, for a *L. hawaiiensis* colony at 90 m depth, located close to Hawaii, average radial extension rates of 1.1

± 0.3 cm per year were measured, which is comparable to some shallow-water corals (Kahng, 2013). Veron (2000) states that extended tentacles have never been observed day or night for *P. speciosa*, suggesting this species is fully autotrophic by creating energy from light, though the irradiance over depth decreases rapidly across mesophotic habitats. This shows that a significant photo-acclimatization is essential for the survival and success of zooxanthellate corals across a large depth gradient as it can be found in MCEs (Kahng *et al.*, 2012). Therefore, it is necessary to understand the photo-physiology of zooxanthellate corals of mesophotic habitats to assess the 'deep reef refugia' hypothesis, and also to provide vital knowledge for resource management of the deep (Hinderstein *et al.*, 2010).

1.4 Hypotheses and research questions

To date, only few studies exist on the photo-physiology and photo-acclimatization of zooxanthellate mesophotic corals across a very large depth gradient. However, most of them are limited to the investigation of only one pigment (chlorophyll *a*) (Nir *et al.*, 2014), narrowed in samples size (*n* = 19) (Kahng *et al.*, 2012) or where restricted to shallower depths (5-40 m) (Frade *et al.*, 2008a), as well as solely greater depths (65-125 m) (Pochon *et al.*, 2015).

In this study, an integrated approach was used to determine the physiological adaptations of depth-generalist coral species (*Leptoseris* spp. and *Pachyseris speciosa*) over a large depth range (10 - 80 m) at Osprey Reef in the Coral Sea to answer following questions:

- **i.** Do the coral genera *Pachyseris* and *Leptoseris* feature similar adaptations for the survival across a large depth gradient?
- **ii.** Do morphological adaptations (skeletal density, tissue thickness and lipid concentrations) occur in mesophotic corals over a large depth range?
- **iii.** Which *Symbiodinium* adaptations (physiology, densities and mitotic indices) are used to cope with the reduced light-availability in deeper habitats?
- **iv.** How does the respective composition of light-harvesting and photoprotective pigments change across a large depth gradient?
- **v.** In which way do the physiological adaptations interact with each other to allow zooxanthellate scleractinian corals to thrive under extreme low-light conditions?

2 Materials and methods

2.1 Sample collection

All samples (*n* = 165) were collected between 22.10.2012 and 26.10.2012 in the Coral Sea at the Osprey Reef (Fig. 1). This reef lies within the borders of the *Coral Sea Commonwealth Marine Reserve* (former: *Coral Sea Conservation Zone*) and forms a steep offshore atoll which is located approximately 180 km off the northeast coast of Australia and about 130 km away from the Great Barrier Reef. At the northwestern part of the reef, three different sample sites were chosen: Osprey 1 [-13.8585, 146.562], Osprey 2 [-13.820333, 146.561167] and Osprey 3 [-13.889333, 146.555]. At each of these sites, sampling was carried out along the extremely steep topography at depths of 10 m, 20 m, 40 m, 60 m and 80 m. Samples from 10 m to 40 m depth were collected by certified scientific SCUBA divers and specimens from below 40 m were collected by a SeaBotix vLBV-300 Remote Operated Vehicle (ROV). An initial identification of the coral species was carried out during the process of sampling, as well as prior to the preservation. In total four zooxanthellate coral species have been collected: *Pachyseris speciosa* (*n* = 84), *Leptoseris scabra* (*n* = 50), *Leptoseris glabra* (*n* = 17) and *Leptoseris hawaiiensis* (*n* = 14). All coral fragments have been photographed and were subsequently 'snap-frozen' in liquid nitrogen (-80°C). Afterwards, the samples were stored in a freezer (-20°C) in anticipation of being processed.

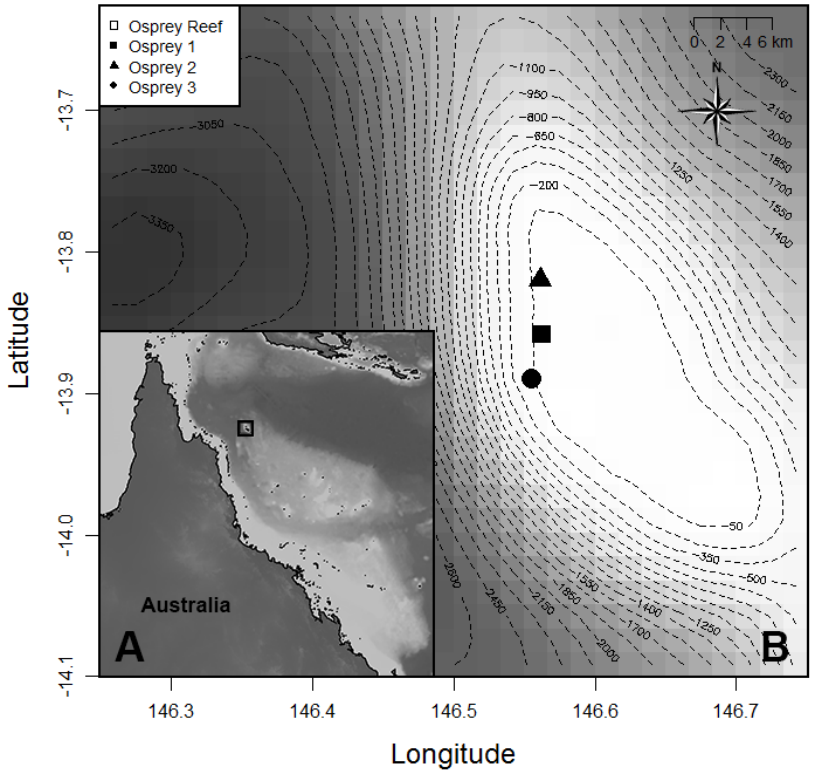

Fig. 1 **A**: Coral Sea along the northeast coast of Australia. Osprey Reef is marked with a black box. **B**: Map of the Osprey Reef with bathymetry [m] and the three sample sites along the northwestern part of the reef.

2.2 Sample processing

2.2.1 Separation of coral skeleton and tissue

Preliminary to further analyses, the coral tissue needed to be extracted from the coral skeleton. Strychar (2002) speculated that using an air-brush to extract symbionts from the tissue may be harmful, which could lead to an elevated amount of dead *Symbiodinium* cells. However, since the samples were kept frozen for more than two years this value was not evaluated. Furthermore, it represents a quick and commonly used procedure (i.e. Dove *et al.*, 2008; Middlebrook *et al.*, 2010). Accordingly, the tissue was removed from the *Symbiodinium* associated (upper) side of the frozen coral fragments by using an air-brush and 10 mL filtered phosphate buffer (0.06 M, pH 6.65), as described by Johannes and Wiebe (1970).

The homogenate was centrifuged (Model: 3K15, Sigma Laboratory Centrifuges, Osterode am Harz, Germany) at 4°C and 4,500 rpm for 5 minutes. The supernatant was transferred into a new tube and kept frozen (-80°C) for host protein analyses. The remaining pellet was resuspended in 3 mL filtered phosphate buffer and separated evenly into three aliquots: symbiont cell counts, pigment quantification with High-performance liquid chromatography (HPLC) and one back-up. All aliquots were stored at -80°C until further processing. For better preservation (recommended by lab manager A. Van den Heuvel), the supernatant of the HPLC and back-up aliquots were removed and only the respective pellets were stored.

In order to clean and conserve the remaining coral skeletons, they were bleached in 20 % hydrogen peroxide for approximately 48 hours in accordance to the standards of the Museum of Tropical Queensland, Townsville. Following, they were rinsed with deionised water and dried in an oven until they reached a steady weight.

2.2.2 Coral skeleton analyses

During the sampling process only preliminary determinations of the species were conducted. Hence, the dried coral skeletons were taxonomically examined to determine all the present species. By using a Nikon SMZ1500 (Tokyo, Japan) stereomicroscope and identification literature (Dinesen, 1980; Veron, 2000) classifications were made. Specimens from deeper habitats displayed typically a more filigree skeleton. Hence, determinations were confirmed by the taxonomists Dr. Zena Dinesen and Dr. Paul Muir.

To make results comparable to other studies it is necessary to normalize the data with the surface area [cm^{-2}] of the *Symbiodinium* associated (upper) side of the coral fragment. There are many different techniques to obtain the surface area: foil wrapping (Marsh, 1970), double and single

paraffin wax dipping (Stimson and Kinzie III, 1991), latex dipping (Meyer and Schultz, 1985), immersion in dye (Hoegh-Guldberg, 1988) and many more. Veal *et al.* (2010) recommended the usage of single paraffin wax dipping for non-branching and minor porous corals, since this is a cheap, quick method with a high accuracy. Accordingly, the dry weights of the coral skeletons were determined three times with an analytical balance (± 0.0001 g) (Model: HR-250AZ, A & D Company Limited, Tokyo, Japan) and then single-dipped in wax at 77°C (Model: Professional Wax Heater, Caronlab Australia Pty Ltd, North Geelong, Victoria, Australia). While still soft, the wax was cut off from sides which were not associated with *Symbiodinium*. As soon as the wax solidified, the skeleton was reweighed three times. As endorsed by Veal *et al.* (2010), a calibration curve of objects with known surface area was generated (n = 15) and the y-intercept calculated. Finally, the surface area of *Symbiodinium* bearing sides was calculated in accordance to Veal *et al.* (2010) (Eq. 1).

$$Surface\ area\ [cm^2] = (mass_{incl.wax}\ [g] - mass_{excl.wax}\ [g]) \cdot intercept[cm^2/g] \qquad \text{Eq. 1}$$

Colony plate thickness was not analysed, since the sample fragments were extremely small (between 3 cm² - 9 cm²). Furthermore, it was not always possible to consider from which section the coral fragment originated (i.e. along the leading edge of the coral colony).

The coral volume and density were determined with the buoyant weight method described by Jokiel *et al.* (1978), which bases on Archimedes principle and is commonly used in coral research (e.g. Davies, 1989; Takabayashi and Hoegh-Guldberg, 1995; Jantzen *et al.*, 2013). The volume of the coral fragment was calculated by using equation Eq. 2 with the density of the used liquid medium (ρ_{water}) (Küster *et al.*, 1972; Davies, 1989). Therefore, the weight of the coral fragment in deionised water and in air was measured three times respectively with an analytical balance (± 0.0001 g) (Model: HR-250AZ, A & D Company Limited, Tokyo, Japan). Afterwards, the results were normalised with the surface area obtained from Eq. 1.

$$Skeleton\ volume\ [cm^3] = \frac{mass_{air}\ [g]\ - mass_{water}\ [g]}{\rho_{water}\ [g/cm^3]} \qquad \text{Eq. 2}$$

The density of the coral fragments was calculated (Eq. 3) via a slightly modified version of equation Eq. 2 by Davies (1989) and afterwards normalised with the surface area (Eq. 1).

$$Skeleton\ density\ [g/cm^3] = \frac{mass_{air}\ [g]\ \cdot\ \rho_{water}[g/cm^3]}{mass_{air}[g]\ - mass_{water}[g]} \qquad \text{Eq. 3}$$

2.2.3 Coral tissue analyses

The *Symbiodinium* densities were determined in accordance to Strychar *et al.* (2005) with a Neubauer Improved Bright-Line hemocytometer (Blaubrand, Wertheim, Germany) and a Olympus BX43 (Tokyo, Japan) light microscope. As recommended by Dove *et al.* (2008), replicate counts (n = 6) were performed on diluted samples. A representative dilution featured a total count of 60 to 80 cells. Furthermore, mitotic cells were counted when paired nuclei or dividing cells were observed (Brown and Zamani, 1993). Following, the *Symbiodinium* counts were normalized with the coral surface area results from Eq. 1.

The *Symbiodinium* sizes were obtained parallel to the cell counts. For this, 30 randomly chosen round and healthy cells were measured using an Olympus BX43 light microscope equipped with an ocular micrometre.

To obtain the total host protein concentration of the samples, the commonly applied method (i.e. Dove *et al.*, 2006; Middlebrook *et al.*, 2010) by Whitaker and Granum (1980) was used. For this, the previously obtained host tissue suspension from the air-brushing procedure (2.2.1) was diluted with filtered phosphate buffer. Afterwards, the difference in absorbance at two different wavelengths (235 nm and 280 nm) was measured by using a SpectraMax M2 Microplate Reader (Molecular Devices Corporation, California, USA). The correct dilution was achieved, when the 235 nm absorbance was smaller than 1.0 and the value at 280 nm showed greater results than 0.1. With the proposed formula (Eq. 4) by Whitaker and Granum (1980) the host protein concentrations were calculated. Whereby, the factor 2.51 represents the difference between the average extinction coefficient at 235 nm and 280 nm.

$$Protein\ conc.\,[mg/mL] = \frac{Absorption_{235\ nm} - Absorption_{280\ nm}}{2.51} \qquad \text{Eq. 4}$$

Subsequently, the total host protein concentrations were standardised to surface area [cm^{-2}] with the results from Eq. 1.

The energy status of the corals were surveyed by determining the total lipid concentrations. Therefore, the modified technique described by Dunn *et al.* (2012) was used, which improved and accelerated the original method of Folch *et al.* (1956). A frozen coral fragment of about 2 cm^2 to 3 cm^2 in size was cleaned at the sides not associated with *Symbiodinium* to prevent elevated results, and then was placed into a gas-tight glass jar. Next, the fragment was covered with 5 mL fresh chloroform:methanol (2:1 v/v) mixture and then was placed in a fridge (4°C) for 16 hours. Thereby, the jar was pivoted time by time to secure extraction also from deeper tissue layers. The suspension was then filtered into a 15 mL reaction tube by using a 0.22 µm hydrophilic PTFE micro syringe filter

(Membrane Solutions, Dallas, Texas, USA). The remaining coral skeleton was dried in an oven and its surface area was calculated as described in Eq. 1. The extracted suspension was then washed by adding 1 mL potassium chloride (0.1 M) and 5 mL methanol:milliQ (1:1 v/v), vortexed and placed in the dark at 4°C for two hours. During this time, the aqueous, middle and organic phases separated (Fig. 2). Next, the aqueous and middle phases were carefully removed and the washing of the remaining organic phase was repeated (three times). Subsequently, the organic phase was poured into pre-weighed (Analytical balance model: HR-250AZ, A & D Company Limited, Tokyo, Japan (± 0.0001 g)) aluminium weighing dishes (LabFriend, Sydney, Australia) and was allowed to evaporate to constant weight. Finally, the mass difference was calculated and the resulting lipid content was standardised to surface area [cm^{-2}] for each fragment.

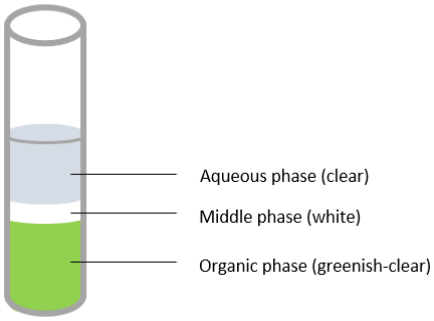

Fig. 2 Reaction tube after two hours at 4°C with three phases: aqueous, middle and organic phase.

The pigment composition within the *Symbiodinium* cells was evaluated by high-performance liquid chromatography (HPLC). The pigments were extracted prior to the analyses in shaded reaction tubes (wrapped in aluminium foil) to prevent degradation of the extracted pigments (recommended by lab manager A. Van den Heuvel). The extractions of the water insoluble host pigments were performed as described by Middlebrook *et al.* (2010). Hence, the frozen (-80°C) pellets from the air-brushing (2.2.1) were resuspended in 2 mL cooled 90% HPLC-grade acetone (with 10% milli-Q water). In derogation from Middlebrook *et al.* (2010) where 100% methanol was used, the usage of 90% acetone is recommended by Latasa *et al.* (2001) and the team of Zapata *et al.* (2000). Accordingly, the usage of 90% acetone as extraction solvent results in much more stable pigments, even over a comparable long time in the solvent (up to 48 hours) and induces much less allomerization (autoxidation) of chlorophylls than methanol. This makes acetone a quite common solvent (e.g. Porra *et al.*, 1989; Humphrey and Jeffrey, 1997; Porra, 2005). However, by using 90% acetone, it is necessary to add a small amount of milli-Q water immediately before the HPLC measurements to avoid peak distortion. This was achieved by programming an autosampler, as recommended by Latasa *et al.* (2001). After the resuspension of the pellets, the reaction tubes were placed in an ultrasonic bath (Model: FXP10DH, Unisonics Pty. Ltd., Sydney, Australia), filled with ice and deionised water, for 10 minutes. Subsequently, the homogenates were spun down (Model: 3K15, Sigma Laboratory Centrifuges, Osterode am Harz, Germany) at 4°C and 5,000 rpm for 5 minutes and the supernatants were poured into new aluminium covered reaction tubes. This process was repeated until the supernatants were clear (in average three times). Next, the recovered supernatants were filtered with 0.22 µm polypropylene syringe filters (Millex-GV, Merck, Darmstadt, Germany) to remove filter and cell debris.

After the extraction, the analysis was performed by using an HPLC system consisted of following parts, manufactured by Shimadzu (Kyōto, Japan): SIL-30AC autosampler, DGU-20A on-line degasser, LC-30AD solvent delivery unit, CTO-10ASVP column oven with a symmetry C_8 column (150 x 4.6 mm, 3.5 µm particle size and 100 Å pore size) (Waters, Milford, USA), SPD-M10AVP diode array detector, RF-10AXL spectrometric detector and a CBM-20A system controller. The HPLC was connected to a personal computer with the installed software LabSolutions LC/GC (Version 5.51) to control and analyse the measurements. Same as Zapata *et al.* (2000) and Dove *et al.* (2006), two mobile phases were used. Eluent A was a methanol:acetonitrile:aqueous pyridine (0.25 M, pH = 5.0) mixture (50:25:25 v:v:v) and eluent B consisted of methanol:acetonitrile:acetone (20:60:20 v:v:v). All organic solvents used in the mobile phase preparations featured HPLC-grade. After loading the precooled autosampler with standards (DHI, Hørsholm, Denmark) and samples, concentrations and elution profiles of light-harvesting and photoprotective pigments were measured at different wavelengths (Fig. 3) using the methodology described by Zapata *et al.* (2000) and Dove *et al.* (2006). As recommended by Latasa *et al.* (2001), immediately prior to the measurements, each sample was diluted by an autosampler with 0.2 mL milli-Q water added per 1 mL of sample to avoid peak distortion. Following, the detected pigment concentrations were normalised to surface area [cm^{-2}], *Symbiodinium* cell [pg $cell^{-1}$] and Chlorophyll *a* [Chl a^{-1}]. Furthermore, the xanthophyll pool per Chl *a* (Dtx + Ddx) Chl a^{-1}) and the ratio of PP to LH ((Ddx + Dtx + *ß*-caro) (Chl *a* + Per + Chl c_2 + Fuco)$^{-1}$) were calculated. The xanthophyll de-epoxidation (Dtx (Dtx + Ddx)$^{-1}$) was not calculated, since the samples were exposed to elevated light levels during the sampling process. Hence, the individual xanthophyll levels are not reliable because diatoxanthin was probably converted to diadinoxanthin by epoxidation (Müller *et al.*, 2001; Frade *et al.*, 2008b).

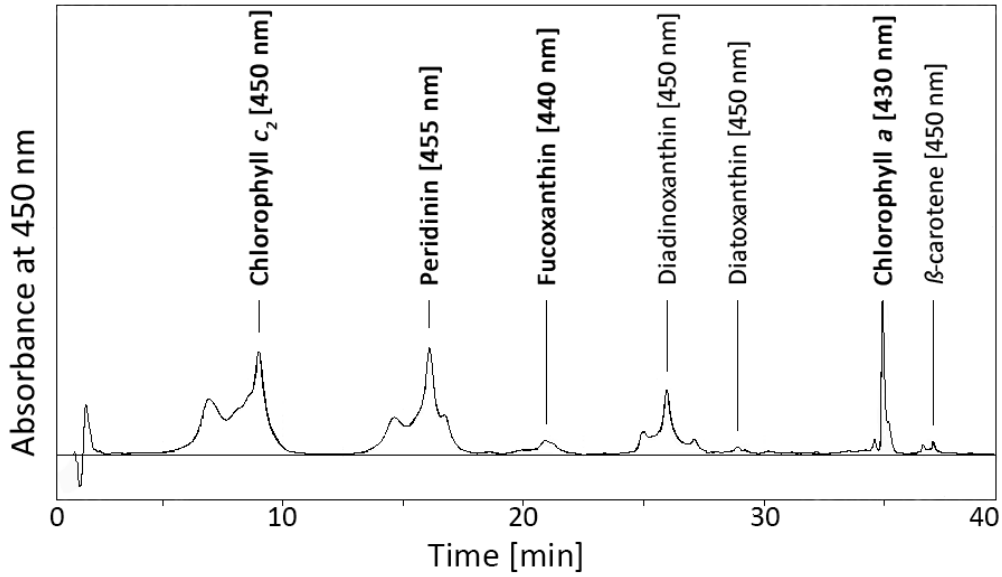

Fig. 3 Typical elution profile measured with a symmetry C_8 column at 450 nm of acetone-soluble light-harvesting (bold) and photoprotective pigments using the methodology of Zapata *et al.* (2000) and Dove *et al.* (2006). In brackets are the respective wavelengths for the correct detection of the concentrations.

2.3 Data analyses

With the software R (version 3.2.0) (R Core Team, 2015) the entire statistical analysis was performed for the four zooxanthellate coral species *Pachyseris speciosa* (*n* = 84)*, Leptoseris scabra* (*n* = 50)*, Leptoseris glabra* (*n* = 17) and *Leptoseris hawaiiensis* (*n* = 14). Since most studies in the literature only provide data on genus level (e.g. Chan *et al.*, 2009; Kahng *et al.*, 2012; Luck *et al.*, 2013; Kahng *et al.*, 2014; Pochon *et al.*, 2015), a fifth group, *Leptoseris* spp. (*n* = 81), was generated by combining all *Leptoseris* samples to allow better comparability.

Prior to other statistical analyses, the dataset was checked for statistically significant differences ($p < 0.05$) between the three sampling locations by using the analysis of variance (ANOVA) to justify whether it is appropriate to pool the variables within the dataset.

As described by Frade *et al.* (2008a) and Lê *et al.* (2008), multiple principal component analysis (PCA) were used to investigate (i) whether the coral genera *Pachyseris* and *Leptoseris* feature similar adaptations for the survival across a large depth gradient (3.2). The PCA is based on the transformation of the dataset into a new coordinate system, while reducing its dimensionality for easier interpretation of the correlations and interactions. Via principal components and graphical correlations, conclusions about interactions can be made.

Correlation analyses of the four coral species and the *Leptoseris* genus were conducted to show in which extent morphological (ii & iii) and pigment (iv) adaptations in mesophotic corals occur across a depth range of 10 to 80 m. In this way, the means of physiological parameters, as well as light-harvesting and photoprotective pigments, were plotted against the depth gradient (3.3). To describe qualitatively the strength and direction of linear associations between the depth and physiological variables, Pearson's correlation coefficient was calculated (Table 2), since it is recommended for linear relationships between each of the variables (Whitlock and Schluter, 2009). The calculation of this correlation coefficient assumes that the variables have a bivariate normal distribution, which was tested via multiple scatter plots (Whitlock and Schluter, 2009). If non-bivariate normality was detected, transformations were performed.

By using the analysis of variance (ANOVA), significant differences between the genera *Pachyseris* and *Leptoseris* (i), as well as the changes of physiological parameters across the water column (ii - iv) were revealed. Since two of the major assumptions of an ANOVA are Gaussian distribution and homogeneity of variance of the dataset (Lewis, 1971; Shaw and Mitchell-Olds, 1993; Milliken and Johnson, 2009; Whitlock and Schluter, 2009), these were tested prior to the analysis in multiple ways. To test whether the dataset was normally distributed Shapiro-Wilk's tests (Shapiro and Wilk, 1965) were conducted, since this test ranks among the most powerful normality tests (Razali and Wah,

2011). In order to verify these results, tests for skewness and kurtosis (Mardia, 1970) were performed. Furthermore, the outlier labelling rule (Tukey, 1977) was used to test for outliers. It consists of taking the difference of the first and third quartile of the data and multiplying it by 1.5 according to Tukey (1977) or by 2.2 according to a revision by Hoaglin and Iglewicz (1987). Afterwards the calculated value was respectively subtracted from the first quartile and added to the third quartile to determine the boundaries for outliers. Finally, parametric Leven's tests (Martin and Bridgmon, 2012) were conducted to assess the homogeneity of variance. Variables which not met these assumptions where transformed, since Hoffmeister *et al.* (2006) recommends a transformation over non-parametric tests because it calculates the *ß*-error more accurate.

Following, F-tests from an ANOVA were used to examine the contribution of each main effect (depth and species) and their interaction. Thereby the ANOVA with type III sums of squares was used, since it is recommended for unbalanced designs (unequal numbers of samples per species and depth) (Shaw and Mitchell-Olds, 1993; Keppel and Wickens, 2004; Milliken and Johnson, 2009). Since the previous ANOVA to justify whether it is appropriate to pool the variables within the dataset indicated certain values as close to the significance threshold ($p < 0.05$), the location was implemented as random factor. Non-significant interactions were dropped to optimize the model and to receive more accurate results for direct comparisons per species and depth (Whitlock and Schluter, 2009).

Statistically significant results reported by the ANOVA, were further analysed with post hoc tests of all possible pairs of means to locate the responsible matches. Accordingly, the Tukey-Kramer test with adjusted p values was carried out since it is one of the most powerful post hoc tests for unbalanced designs since its probability of making at least one type I error is no greater than the chosen significance level (Dunnett, 1980; Hsu, 1996; Whitlock and Schluter, 2009).

The ANOVA was followed by multiple principal component analysis (PCA) (3.4). Each coral species, as well as the genus *Leptoseris*, was investigate in combination with depth to reveal (v) in which way all physiological parameters of a certain species interact with each other to allow the successful growth across a large depth gradient.

3 Results

3.1 Three sample sites – One pooled location

An analysis of variance (ANOVA) justified that it is appropriate to pool the different variables of the three sample sites (Fig. 1), since no statistically significant differences ($p < 0.05$) were detected. In this way, all following analyses were made, considering the western side of the Osprey Reef as one sampling location.

3.2 Differences between the coral genera *Pachyseris* and *Leptoseris*

In order to investigate whether the scleractinian coral genera *Pachyseris* and *Leptoseris* have similar strategies to occupy reefs across a large depth gradient (i), a mixed-design ANOVA was conducted. A comparison between *Pachyseris* sp. and *Leptoseris* spp. revealed that almost all parameters, except fucoxanthin [Chl a^{-1}] and the mitotic index, showed statistically significant differences. Thereby, the most significant differences were given by coral skeleton density [$F(1, 169.055) = 94.67$, $p < 0.001$], chlorophyll c_2 [Chl a^{-1}] [$F(1, 169.055) = 193.00$, $p < 0.001$] and β-carotene [Chl a^{-1}] [$F(1, 169.055) = 68.58$, $p < 0.001$]. The least statistically significant differences represented peridinin [Chl a^{-1}] [$F(1, 169.055) = 4.70$, $p = 0.03$], and diadinoxanthin [Chl a^{-1}] [$F(1, 169.055) = 8.16$, $p = 0.005$]. Investigated on species level, similar pattern were observed between *P. speciosa* and each *Leptoseris* species. By taking the interaction between water depth and species into account, several statistically significant differences between *Pachyseris* sp. and *Leptoseris* spp. were detected. Thereby, especially the lipid [$F(1, 170.711) = 13.96$, $p < 0.001$] and protein [$F(1, 161.256) = 4.68$, $p = 0.03$] concentrations, as well as the *Symbiodinium* size [$F(1, 170.792) = 10.70$, $p = 0.001$] featured statistically significant interactions.

Via a principal component analysis (Fig. 4) and correlation analyses (Table 2) these observations were confirmed. Altogether, 165 samples (*P. speciosa* ($n = 84$), *L. scabra* ($n = 50$), *L. hawaiiensis* ($n = 14$), *L. glabra* ($n = 17$)) with 24 variables (Table 1) and three explanatory variables (species, depth and location) were included in the PCA (Fig. 4). The exclusion of pigments normalized to *Symbiodinium* cell density did not lead to an improvement of the variance as reported for other PCAs in chapter 3.4 for *Pachyseris speciosa* or *Leptoseris* spp., hence the entire dataset was used. The active and explanatory variables were used to calculate the correlations within the principal components (PCs). Thereby, the first six PCs displayed a variance greater than 1 and accounted together for 75.3% of the variation (27.2%, 17.8%, 12.1%, 7.8%, 5.3% and 5.1%, respectively) and were therefore used for further investigations. As it can be seen in Table 1, the only variable which featured statistically significant correlations ($p < 0.05$) in all six PCs was the explanatory variable Depth. This was followed by *Symbiodinium* cell density, chlorophyll *a* [µg cm^{-2}], lipid concentration, skeletal density, as well as

the explanatory variable Species, with respectively five statistically significant correlations within the six PCs. Ratios of *ß*-carotene [Chl a^{-1}], which were also statistically significant according to a previous mixed-design ANOVA, displayed in four of six cases statistically significant correlations in the PCs. The smallest overall correlation of active variables was represented by peridinin [pg $cell^{-1}$], though it shows a significantly positive correlation in the first PC. The smallest overall correlation (at five of six PCs) of an explanatory variable featured the Location (Table 1). This supports that it is appropriate to pool the different variables of the three sample sites, which was tested before (3.1).

Only the first two principal components (cumulative variance 45.0%) are displayed in Fig. 4 A & B, since the other PCs respectively only represent 12.1%, 7.8%, 5.3% and 5.1% of the variance. It can be seen that *P. speciosa* is the only species in the upper left quartile (Fig. 4 A), because it is more correlated to the protein concentration, chlorophyll c_2 [Chl a^{-1}] and *ß*-carotene [pg $cell^{-1}$] (Fig. 4 B). This was also reported by ANOVA and pairwise comparisons (3.3). Due to these correlations, *P. speciosa* is graphically and statistically significantly (ellipse inclosing a confidence interval of 95%) separated from all three *Leptoseris* species (*L. scabra*, *L. glabra* and *L. hawaiiensis*). Likewise it can be seen that the elliptical confidence intervals of these three *Leptoseris* species overlap, so *L. scabra*, *L. glabra and L. hawaiiensis* are not statistically significant different from each other and can be therefore legitimately combined to *Leptoseris* spp. (note: In Fig. 4 A no data points are displayed for *Leptoseris* spp. since they would overlap the respective *Leptoseris* species. Only a dark blue ellipse, inclosing a confidence interval of 95%, is displayed.). Hence, a statistically significant difference ($p < 0.05$) can be observed for the coral genera *Pachyseris* and *Leptoseris* (i).

Table 1 Species composition correlations and percentages of cumulative variances for the first six principal components (PC) created by the principal component analysis (PCA). Explanatory variables are shown in parenthesis and significant correlations ($p < 0.05$) in bold. The table is sorted by the correlations of PC 1. PP/LH represents the ratio between photoprotective and light-harvesting pigments.

Variables	**PC 1**	**PC 2**	**PC 3**	**PC 4**	**PC 5**	**PC 6**
Symbiodinium cells [10^6 cm^{-2}]	**-0.63**	**0.20**	**0.36**	**-0.23**	**0.28**	-0.07
Chlorophyll c_2 Chl a^{-1}	**-0.48**	**0.49**	**-0.19**	0.03	0.15	**0.32**
ß-carotene [pg cell^{-1}]	**-0.47**	**0.72**	0.13	**-0.20**	-0.12	**-0.21**
Protein [mg cm^{-2}]	**-0.45**	**0.21**	**0.34**	0.12	0.11	**0.55**
(Species)	**-0.45**	**0.38**	-0.05	**-0.25**	**0.23**	**0.21**
ß-carotene Chl a^{-1}	-0.11	**0.81**	**0.25**	**-0.30**	-0.04	**-0.16**
Symbiodinium size [µm]	-0.10	**0.29**	**0.36**	-0.01	**-0.31**	**0.41**
Diatoxanthin Chl a^{-1}	-0.08	**0.76**	0.05	**0.55**	0.07	**-0.21**
PP/LH	-0.01	**-0.78**	**0.38**	**0.30**	0.07	-0.04
(Location)	0.02	-0.06	0.09	-0.04	**0.26**	-0.07
Fucoxanthin Chl a^{-1}	0.05	**-0.24**	**-0.26**	**0.53**	**0.44**	0.12
Xanthophyll pool Chl a^{-1}	0.10	**0.55**	**-0.78**	-0.04	-0.09	0.08
Diadinoxanthin Chl a^{-1}	0.12	**0.45**	**-0.83**	-0.13	-0.10	0.12
(Depth [m])	**0.22**	**-0.23**	**-0.29**	**-0.25**	**0.50**	**-0.23**
Peridinin Chl a^{-1}	**0.24**	0.08	**-0.50**	**0.24**	-0.08	-0.12
Lipid [mg cm^{-2}]	**0.30**	**-0.19**	**0.33**	**0.16**	**-0.56**	0.02
Chlorophyll *a* [µg cm^{-2}]	**0.32**	**0.31**	**0.57**	**-0.36**	**0.21**	-0.06
Mitotic index	**0.32**	0.03	-0.04	**-0.22**	0.00	**0.26**
Skeletal density [g cm^{-3}]	**0.38**	**-0.26**	-0.12	**0.18**	**-0.44**	**-0.28**
Chlorophyll *a* / Protein	**0.61**	0.05	0.12	**-0.35**	0.07	**-0.43**
Diatoxanthin [pg cell^{-1}]	**0.61**	**0.60**	**0.17**	**0.40**	0.00	-0.08
Fucoxanthin [pg cell^{-1}]	**0.90**	-0.01	0.07	**0.18**	**0.26**	0.14
Chlorophyll *c2* [pg cell^{-1}]	**0.93**	**0.21**	**0.17**	-0.06	0.04	**0.17**
Diadinoxanthin [pg cell^{-1}]	**0.94**	**0.23**	-0.03	-0.11	0.02	0.14
Chlorophyll *a* [pg cell^{-1}]	**0.95**	0.11	**0.19**	-0.06	0.03	0.13
Peridinin [pg cell^{-1}]	**0.95**	0.14	0.08	0.01	0.03	0.09
Cumulative variance [%]	27.2	45	57.1	64.9	70.2	75.3

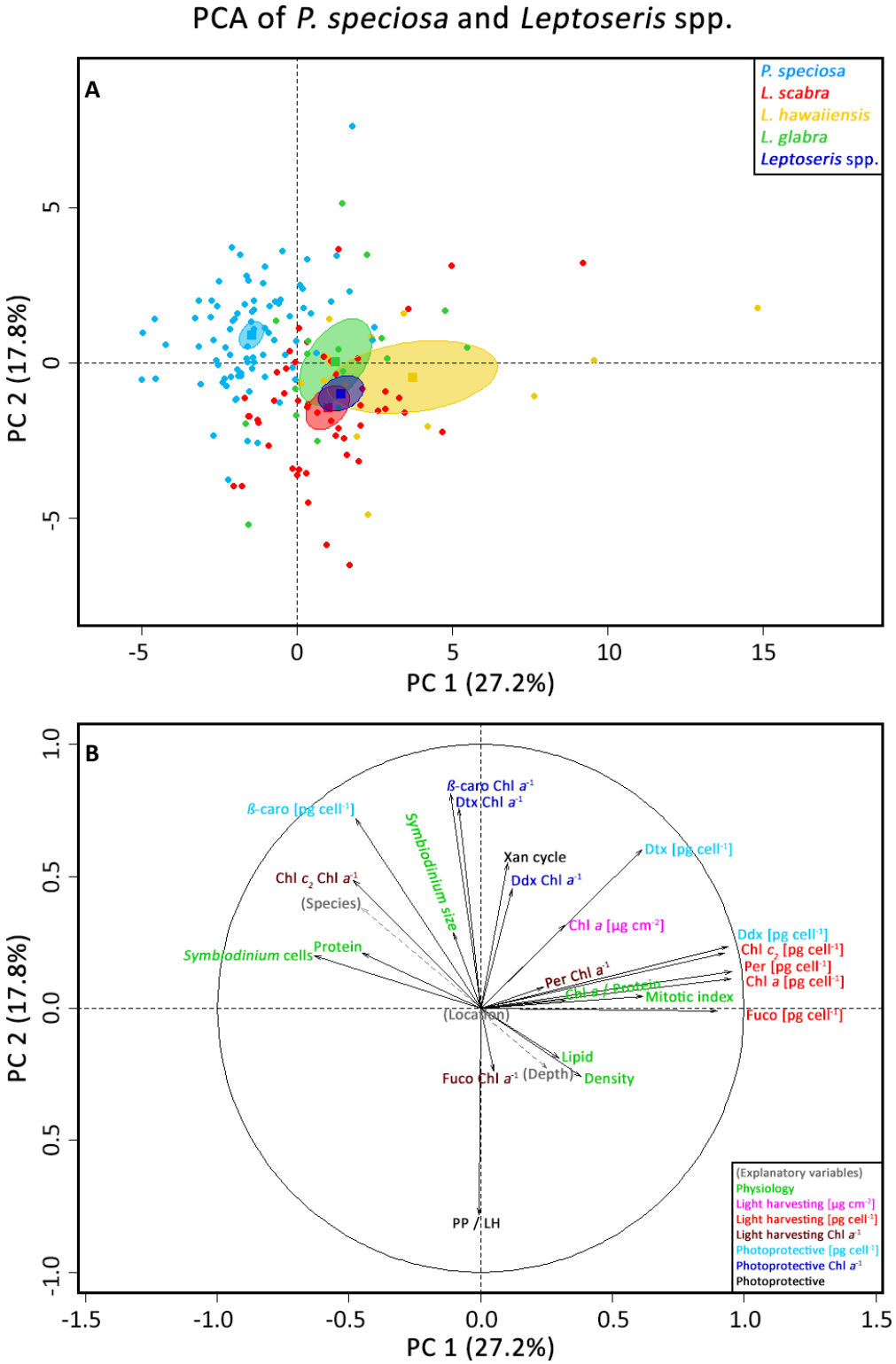

Fig. 4 Principal component analysis (PCA) comparing *Pachyseris speciosa, Leptoseris scabra, Leptoseris hawaiiensis* and *Leptoseris glabra*. **(A)** Individuals graph of the first two principal components (PC) which explains 45.0% of the entire dataset. Ellipses enclose a confidence interval of 95% around the respective mean (square) of a species. **(B)** Variables graph of the first two principal components (PC) which explains 45.0% of the entire dataset. Concentrations of physiological parameters normalized to surface area are shown in green. Displayed in a colour gradient are light-harvesting (shades of red) and photoprotective (shades of blue) pigments normalized to µg per area (µg cm^{-2}), pg per *Symbiodinium* cell (pg $cell^{-1}$) and chlorophyll *a* (Chl a^{-1}). Explanatory variables are shown in parenthesis. Abbreviations: Chl *a* – Chlorophyll *a*, Per – Peridinin, Fuco – Fucoxanthin, Ddx – Diadinoxanthin, Dtx – Diatoxanthin, Chl c_2 – Chlorophyll c_2, ß-caro – ß-carotene, Xan cycle – xanthophyll pool per Chl *a* (Dtx + Ddx) Chl a^{-1}), PP/LH – ratio of photoprotective to light-harvesting pigments.

3.3 Correlation between water depth and physiological parameters

In order to assess how the concentrations of physiological parameters of zooxanthellate corals change from 10 to 80 m depth (ii - iv) correlation analyses were performed. Table 2 shows a summary of Pearson's correlation coefficient with statistically significant ($p < 0.05$) associations in bold. It can be seen that, *P. speciosa* as well as all three *Leptoseris* species combined to *Leptoseris* spp., equally featured the highest number (six) of statistically significant correlations with the depth. However, both only had two significances in common, namely *ß*-carotene [pg cell^{-1}] and lipid [mg cm^{-2}] concentration. In contrast, *L. glabra*, the only species with no samples from 80 m, displayed no statistically significant correlations with the depth.

Overall, the physiological parameters with the highest significant (positive and negative) correlation coefficients across all five corals are *ß*-carotene [pg cell^{-1}], *Symbiodinium* size [µm] and the lipid [mg cm^{-2}] concentration.

Table 2 Pearson's correlation coefficients between depth (10 - 80 m) and physiological parameters of *Pachyseris speciosa* (*n* = 84), *Leptoseris scabra* (*n* = 50), *Leptoseris glabra* (*n* = 17), *Leptoseris hawaiiensis* (*n* = 14) and *Leptoseris* spp. (*n* = 81). Significant correlations ($p < 0.05$) in bold.

Variables	***P. speciosa***	***L. scabra***	***L. glabra***	***L. hawaiiensis***	***L.* spp.**
Protein [mg cm^{-2}]	**-0.38**	0.09	-0.04	-0.45	-0.12
ß-carotene [pg cell^{-1}]	**-0.34**	-0.13	-0.20	**-0.60**	**-0.26**
Chlorophyll c_2 Chl a^{-1}	**-0.28**	-0.01	-0.30	-0.27	-0.06
Diatoxanthin Chl a^{-1}	**-0.24**	-0.09	-0.08	**-0.71**	-0.16
ß-carotene Chl a^{-1}	**-0.24**	-0.13	-0.26	-0.41	-0.15
Symbiodinium size [µm]	-0.21	**-0.47**	-0.30	**-0.87**	**-0.53**
Diatoxanthin [pg cell^{-1}]	-0.15	-0.19	-0.07	-0.08	-0.06
Symbiodinium cells [10^6 cm^{-2}]	-0.14	0.00	-0.17	-0.53	-0.14
Chlorophyll *a* [µg cm^{-2}]	-0.12	-0.14	-0.23	0.09	0.03
Fucoxanthin Chl a^{-1}	-0.07	0.16	0.27	-0.10	0.08
Xanthophyll pool Chl a^{-1}	-0.02	0.11	-0.17	0.14	0.14
Chlorophyll c_2 [pg cell^{-1}]	-0.01	-0.18	-0.04	0.39	0.18
Fucoxanthin [pg cell^{-1}]	0.00	-0.01	0.14	0.39	**0.23**
Mitotic index	0.01	-0.11	0.28	0.33	**0.22**
Diadinoxanthin Chl a^{-1}	0.02	0.12	-0.16	0.24	0.17
Peridinin Chl a^{-1}	0.03	0.25	-0.37	-0.19	0.14
Chlorophyll *a* [pg cell^{-1}]	0.04	-0.17	0.00	0.39	0.19
Diadinoxanthin [pg cell^{-1}]	0.06	-0.14	-0.08	0.42	**0.23**
Peridinin [pg cell^{-1}]	0.06	-0.10	-0.09	0.37	0.22
Density [g cm^{-3}]	0.11	**-0.37**	-0.08	0.46	-0.10
PP/LH	0.12	0.03	0.17	-0.04	-0.03
Chlorophyll *a* / Protein	0.16	-0.23	-0.21	0.47	0.10
Lipid [mg cm^{-2}]	**0.22**	**-0.40**	-0.34	-0.17	**-0.35**

Graphical correlation analyses of statistically significant results, as well as all major variables, are displayed in Fig. 5 to 7 to support and visualise the correlation coefficient results presented in Table 2. Furthermore, multiple analysis of variance (ANOVA) were performed to investigate significant differences across the depth range. Reported significant differences were further analysed with Tukey-Kramer post hoc tests to locate the responsible significant differences across the depth gradient and are illustrated in the graphs as letters.

Means of physiological parameters in correlation with the depth are shown in Fig. 5. The *Symbiodinium* cell densities per surface area featured slightly downwards trends with increasing depth (Fig. 5 A). For *P. speciosa*, the density almost dropped to the half between 10 m (mean ± SE) (1.09 ± 0.07 10^6 cm^{-2}) and 80 m (0.65 ± N/A 10^6 cm^{-2}). However, only one sample was available for 80 m and furthermore, neither the correlation coefficient, nor the ANOVA declared the decline of the *Symbiodinium* cell density of any species over depth as statistically significant.

The relative correlation of *Leptoseris* spp., as well as each *Leptoseris* species, between *Symbiodinium* cell diameter and depth (displayed in Table 2) was also visible in the graph (Fig. 5 B). The strongest decrease in size over depth showed *L. hawaiiensis* with a mean size of 10.65 ± 0.13 µm at 10 m and 9.13 ± 0.14 µm at 80 m, which was confirmed by Tukey-Kramer pairwise comparisons as statistically significant. Likewise, *Leptoseris* spp. displayed a strong graphical and statistical correlation with depth. The lipid concentration featured graphically only for the *Leptoseris* groups a decrease over depth (Fig. 5 D) and statistically significant only for *Leptoseris* spp. and *L. scabra*. In contrast, the biomass (protein concentration) of *P. speciosa* was the only one which featured a strong linear decline with greater depth (Fig. 5 F), as indicated by the correlation coefficient (Table 2) and pairwise comparisons. The ratio between chlorophyll *a* and proteins showed for all groups, except *L. scabra*, a doubling between 10 and 80 m (Fig. 5 E). However, neither Pearson's correlation coefficient, nor Tukey-Kramer post hoc tests indicated significances. According to pairwise comparisons, as well as the graphical correlation, the density of the different coral skeletons displayed no linear association with the depth gradient (Fig. 5 C). Only samples of *L. scabra* (n = 2) from 80 m showed a reduction in density, which results in a significant correlation coefficient (Table 2).

In Figure 6 the mean concentrations of light-harvesting pigments are presented. According to Pearson's correlation coefficient, only chlorophyll c_2 [Chl a^{-1}] (for *P. speciosa*) (Fig. 6 D) and fucoxanthin [pg $cell^{-1}$] (for *Leptoseris* spp.) (Fig. 6 C) featured statistically significant correlations with depth (Table 2). In the graphs, this was only visible for chlorophyll c_2 [Chl a^{-1}], which was supported by a Tukey-Kramer post hoc test. Further positive depth associations were visible for chlorophyll *a* [pg $cell^{-1}$] (Fig. 6 B), though not when normalized to surface area (Fig. 6 A). Peridinin [Chl a^{-1}] displayed quite different results. While the concentrations decreased with depth for *L. hawaiiensis* and

L. glabra (only the latter one featured statistically significant differences according to Tukey-Kramer), it slightly increased for *P. speciosa* and *L. scabra* (Fig. 6 F).

Photoprotective pigments and the xanthophyll pool [Chl a^{-1}] are displayed in Fig. 7. In total, *P. speciosa* (*n* = 84) and *L. scabra* (*n* = 50), the species with the respectively highest amount of samples, featured the smoothest graphical correlations across the depth gradient. In contrast, *L. hawaiiensis* (*n* = 14) showed quite nonlinear correlations, especially for diatoxanthin [Chl a^{-1}]. Due to this nonlinearity, it featured statistically significant differences between the depths (Fig. 7 B). Graphical correlations for *ß*-carotene ([Chl a^{-1}] and [pg cell^{-1}]) indicated *P speciosa* as strongly associated with depth (Fig. 7 C & D), which is supported by Pearson's correlation coefficient (Table 2) and Tukey-Kramer post hoc tests. However, both *ß*-carotene concentrations were very close to the detection limit of the high-performance liquid chromatography sensor.

In summary, it was possible to show via correlation analyses and pairwise comparisons that zooxanthellate scleractinia corals feature morphological adaptations (change in protein and lipid concentration) to conquer reefs across a large depth gradient (ii). Statistically significant correlations between the depth and the protein concentration were exclusively observable for *Pachyseris speciosa* (*n* = 84). Statistically significant changes of the lipid concentration have been shown for *Leptoseris scabra* (*n* = 50), as well as the coral genus *Leptoseris* (*n* = 81). Physiological and quantitative *Symbiodinium* adaptations to cope with the reduced light-availability in deeper habitats (iii) were observed for *Leptoseris* spp., *Leptoseris hawaiiensis* (*n* = 14) and *P. speciosa*. Thereby only graphical correlations for *Symbiodinium* cells [10^6 cm^{-2}] were found for *P. speciosa*, while strong statistically significant correlations and pairwise comparisons were found for the *Symbiodinium* cell size of the two first mentioned groups. Furthermore, a change in the composition of light-harvesting and photo-protective pigments along a large depth gradient have been found (iv). *P. speciosa* featured the highest amount of statistically significant differences and correlations of light-harvesting (chlorophyll c_2 [Chl a^{-1}]) and photoprotective pigments (*ß*-carotene (both, normalized to chlorophyll *a* and pg cell^{-1})). This was followed by *L. hawaiiensis*, which only showed significant differences among the photoprotective pigment diatoxanthin [Chl a^{-1}]. Finally, the *Leptoseris glabra* (*n* = 17) displayed as only species significant differences across the water column for peridinin [Chl a^{-1}].

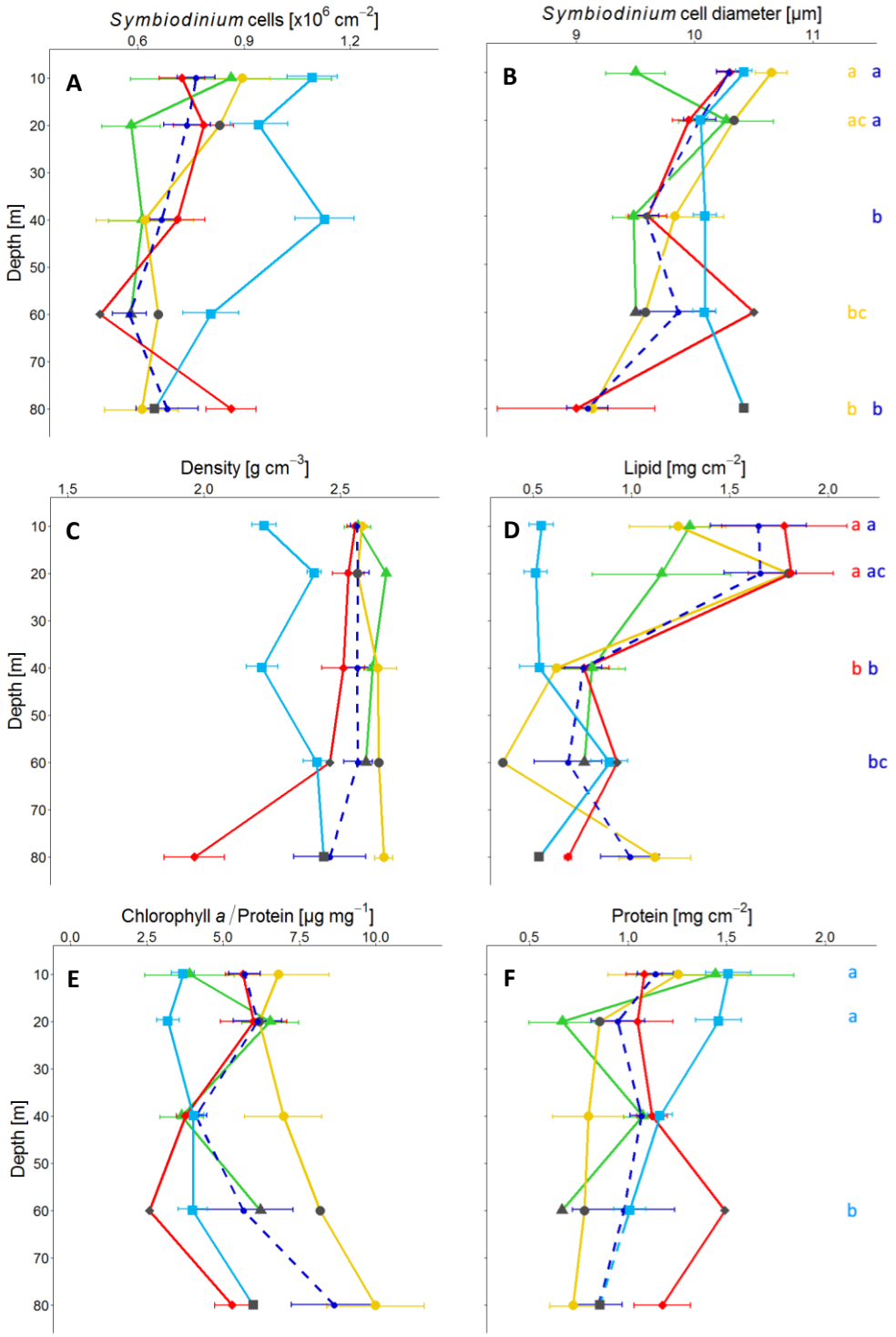

Fig. 5 **(A - F)** Physiological parameter of *Leptoseris* spp. and *Pachyseris speciosa* across a depth gradient (10 - 80 m). Symbols represent means (± one standard error) of *P. speciosa* (, *n* = 84), *L. scabra* (, *n* = 50), *L. hawaiiensis* (, *n* = 14), *L. glabra* (, *n* = 17) and all three *Leptoseris* species combined to *Leptoseris* spp. (, *n* = 81). Data are normalized to surface area, if applicable. Depths with one available sample are indicated in grey. Different letters of the respective group colour are assigned to means with significantly different ($p < 0.05$) Tukey-Kramer post hoc results. Means are not significantly different, if they share the same letter. Means with no letters display no significant differences to any other means.

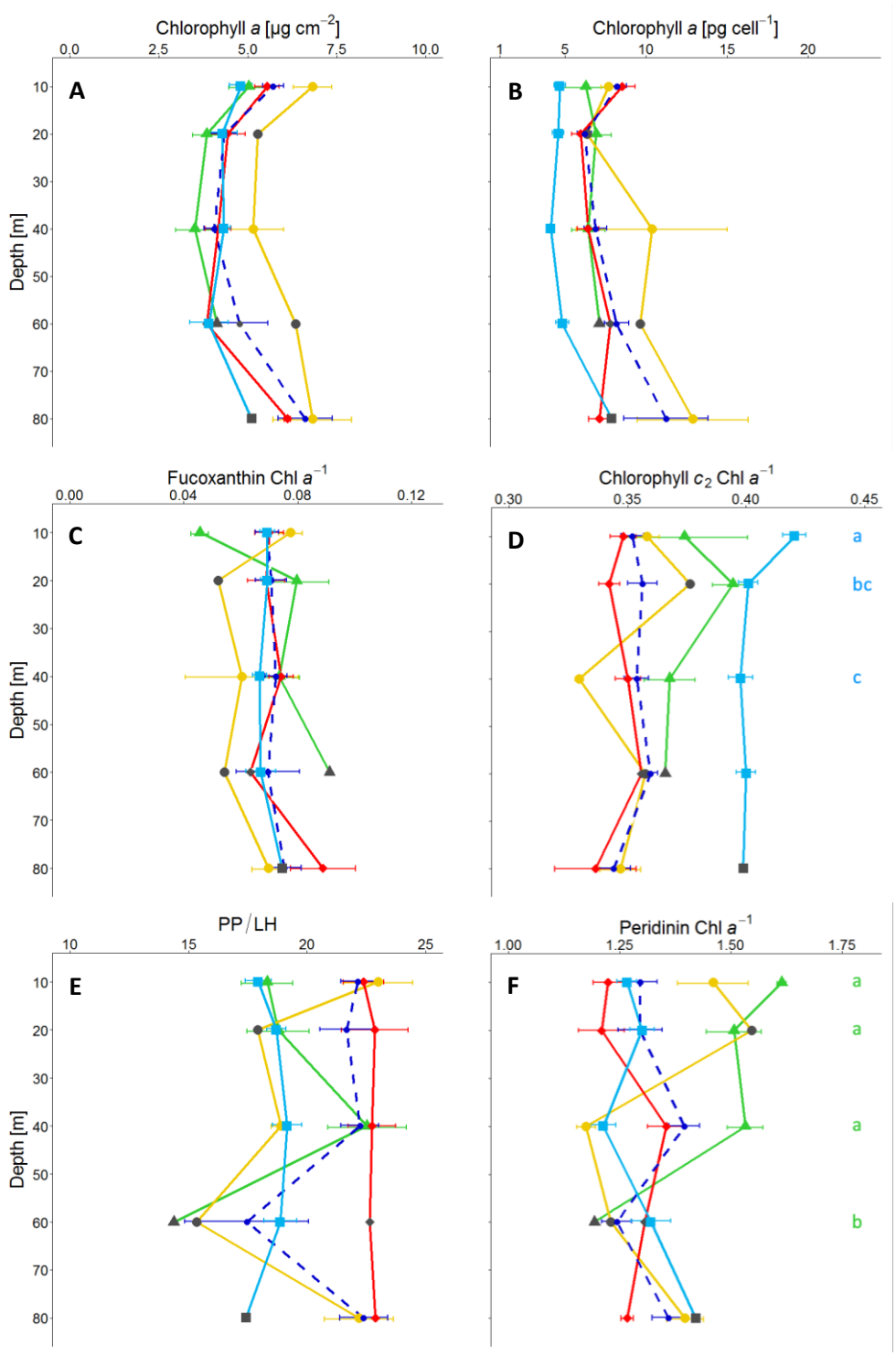

Fig. 6 **(A - F)** Light-harvesting pigments of *Leptoseris* spp. and *Pachyseris speciosa* across a depth gradient (10 - 80 m). Symbols represent means (± one standard error) of *P. speciosa* (, *n* = 84), *L. scabra* (, *n* = 50), *L. hawaiiensis* (, *n* = 14), *L. glabra* (, *n* = 17) and all three *Leptoseris* species combined to *Leptoseris* spp. (, *n* = 81). Depths with one available sample are indicated in grey. The samples were processed using the methodology of Zapata *et al.* (2000) and Dove *et al.* (2006) and normalized to µg per area, pg per *Symbiodinium* cell and chlorophyll *a* concentration. The ratio of photoprotective to light-harvesting (PP/LH) pigments was calculated. Different letters of the respective group colour are assigned to means with significantly different ($p < 0.05$) Tukey-Kramer post hoc results. Means are not significantly different, if they share the same letter. Means with no letters display no significant differences to any other means.

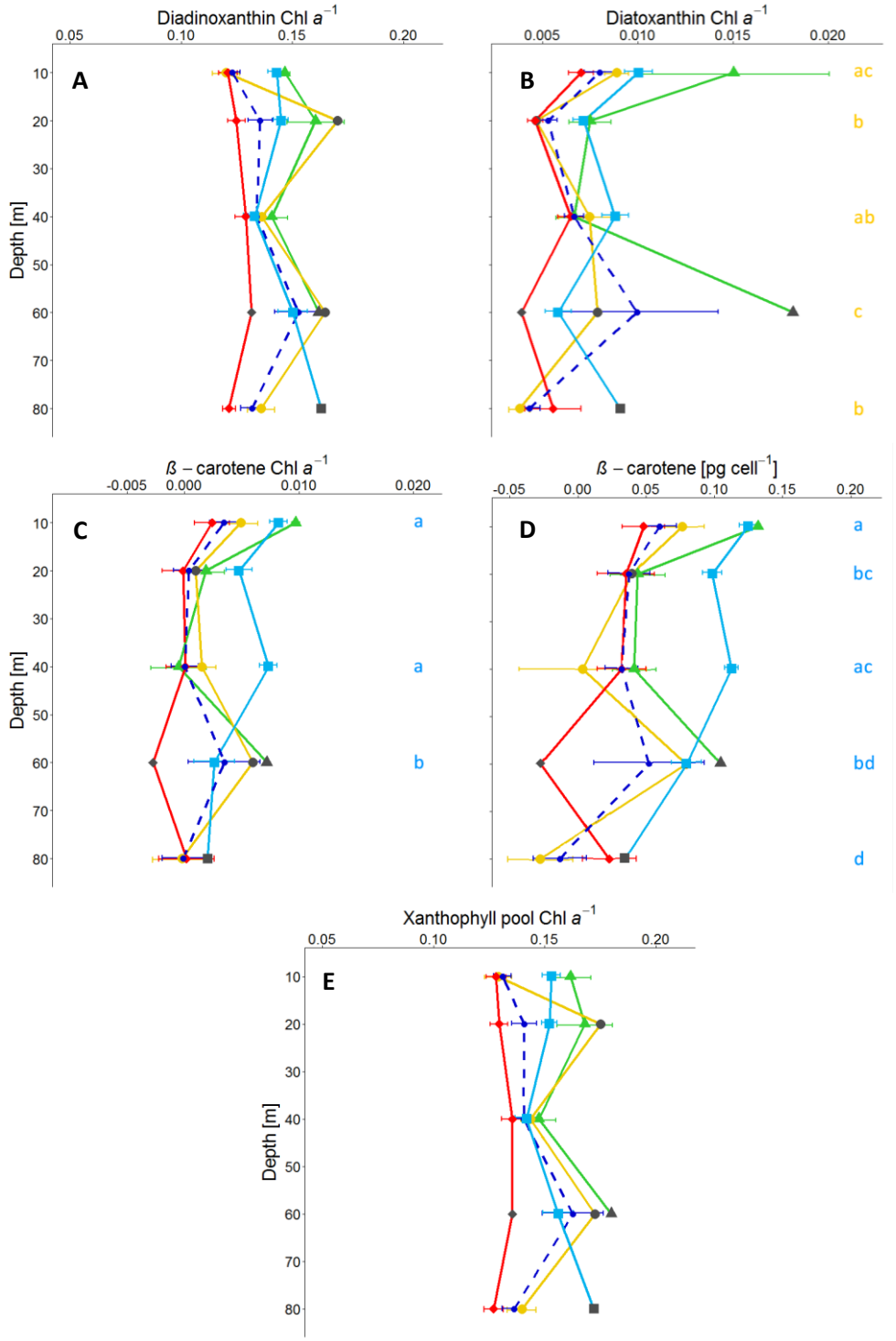

Fig. 7 **(A - F)** Photoprotective pigments of *Leptoseris* spp. and *Pachyseris speciosa* across a depth gradient (10 - 80 m). Symbols represent means (± one standard error) of *P. speciosa* (, *n* = 84), *L. scabra* (, *n* = 50), *L. hawaiiensis* (, *n* = 14), *L. glabra* (, *n* = 17) and all three *Leptoseris* species combined to *Leptoseris* spp. (, *n* = 81). Depths with one available sample are indicated in grey. The samples were processed using the methodology of Zapata *et al.* (2000) and Dove *et al.* (2006). Pigment concentrations and xanthophyll pool (diadinoxanthin + diatoxanthin) were normalized to chlorophyll *a* (Chl a^{-1}). Different letters of the respective colour are assigned to means with significantly different ($p < 0.05$) Tukey-Kramer post hoc results. Means are not significantly different, if they share the same letter. Means with no letters are not significantly different to other means.

3.4 Interactions of physiological parameters in association with the water depth

The correlation of physiological adaptations across a large depth gradient (10 – 80 m) (v) was investigated by multiple principal component analysis (PCA). Since a mixed-design ANOVA and a PCA (3.2) indicated statistically significant differences between *Pachyseris speciosa* and the coral genus *Leptoseris* spp., separate PCAs were conducted for these groups to examine respective adaptations. Prior to these PCAs, the dataset was modified to increase the interpretability by reducing the amount of included variables. Pairwise comparisons and correlation analyses identified previously (3.3) pigment concentration normalized to *Symbiodinium* density as not statistically significant with the depth gradient. By excluding these variables from the PCA for *P. speciosa* (Table 3 A & Fig. 8), for the first and second principal component (PC), a cumulative variance increase of 12.8% was achieved (complete dataset = 47.7% cumulative variance of PC 1 and PC 2, modified dataset = 60.5% cumulative variance of PC 1 and PC 2). By excluding pigments normalized to *Symbiodinium* density for the *Leptoseris* spp. PCA (Table 3 B & Fig. 9), principal component one and two displayed together 5.9% more variance (complete dataset = 35.5% cumulative variance of PC 1 and PC 2, modified dataset = 41.4% cumulative variance of PC 1 and PC 2).

3.4.1 Interactions of physiological parameters of *P. speciosa* and depth

For the investigation of possible adaptations of *P. speciosa* across the depth gradient in total 84 samples and 18 variables were used. Since a variance greater than 1 was represented by the first three principal components, only these are displayed in Table 3 A and Fig. 8 B. Overall, the greatest positive correlations were observable for *ß*-carotene [Chl a^{-1}], chlorophyll c_2 [Chl a^{-1}] and the xanthophyll pool [Chl a^{-1}]. The first two variables were also statistically significant ($p < 0.05$) during pairwise analyses across the depth gradient (3.3, Fig. 6 & 7). In contrast, the last mentioned xanthophyll pool Chl a^{-1} was only significant in PC 1. In PC 2 and 3 it belonged to the variables with the weakest correlation and therefore no statistical significance. Declared as statistically significant correlation ($p < 0.05$) within the first three PCs were chlorophyll *a* [µg cm^{-2}], fucoxanthin [Chl a^{-1}], diatoxanthin [Chl a^{-1}] and the ration of photoprotective to light-harvesting pigments (Table 3 A). The variables with the weakest correlation within all three principal components were the lipid concentration, as well as the skeletal density.

In Fig. 8 the first two PCs (cumulative variance 60.5%) are displayed. The individuals graph (Fig. 8 A) shows *P. speciosa* at different depths (10 m (*n* = 24), 20 m (*n* = 25), 40 m (*n* = 23), 60 m (*n* = 11) and 80 m (*n* = 1)) and ellipses enclosing a confidence interval of 95% around the respective depth mean. It can be seen that a close connection between the different depths existed. Thereby, the confidence ellipses of 10 m and 40 m show a strong interaction, while 20 m only overlaps with 40 m and 60 m. The single sample from 80 m is in close range to the 60 m confidence interval, but due to the lack of

further samples, there is only room for tentative interpretations. When comparing the contents in the quartiles of Fig. 8 A and B, it can be seen which variables are correlated with respective depths. Since the deeper habitats are predominantly located in the lower (right) quartile of Fig. 8 B it can be concluded that a positive correlation with depth occurred for fucoxanthin Chl a^{-1} and skeletal density. The negative sign in front of *Symbiodinium* cells [10^6 cm^{-2}] and the protein concentration in Table 3 A imply a negative correlation, since both form a straight line from the confidence intervals of deeper habitats (Fig. 8 A). Because these two parameters point in the same direction and almost overlap each other, they are furthermore highly positive correlated towards each other. In a reduced extend this accounts also for the chlorophyll *a* concentration per surface area, since it likewise has a negative correlation towards the depth. Though the chlorophyll c_2 concentration normalized to chlorophyll *a* showed similar features, it only has a very short arrow and is therefore not correlative towards any variables. In contrast, the *Symbiodinium* size has neither a correlation with *Symbiodinium* cell density and protein concentration, nor a high correlation with greater depths, since it lays in a 90° angle towards all these features. The same accounts for diatoxanthin [Chl a^{-1}].

In summary, *Symbiodinium* cell density and protein concentration had strong negative correlations with deeper areas. The composition of photoprotective pigments (blue) seem to play a slightly greater role than light-harvesting pigments (red).

3.4.2 Interactions of physiological parameters of *Leptoseris* spp. and depth

Several principal component analyses were made for the different *Leptoseris* species. Since all of them showed relatively similar results, and due to the improved interpretability with more samples, only the PCA for *Leptoseris* spp. (*n* = 81) will be reported. A variance greater than 1 was represented of the first five principal components (cumulative variance = 71.7% build of 24.1%, 17.3%, 12.1%, 9.9% and 8.3% variance per principal component), so only these were considered. The first two PCs (cumulative variance 41.4%) are shown in Fig. 8 A (10 m (*n* = 24), 20 m (*n* = 21), 40 m (*n* = 26), 60 m (*n* = 3) and 80 m (*n* = 7)) and the respective correlations of the variables in Table 3 B and Fig. 9 B. Statistically significant and very strong correlations were observable for the explanatory variable Depth across four of five principal components (Table 3 B). Same accounted for the active variable diatoxanthin [Chl a^{-1}], which was also reported by ANOVA and post hoc tests (3.3 & Fig. 7 B). Further, peridinin [Chl a^{-1}] and the ratio of photoprotective to light-harvesting pigments featured statistically significant positive correlations, while *ß*-carotene [Chl a^{-1}] showed significant negative correlations. The lipid concentration, *Symbiodinium* size, chlorophyll c_2 [Chl a^{-1}] and chlorophyll *a* [µg cm^{-2}] displayed the overall strongest correlations in two of five PCs. The weakest overall correlation was given by the protein concentration.

The quartiles in Fig. 9 A & B indicate which variables are correlated with respective depths. In Fig. 9 A it can be seen that almost all elliptic confidence intervals (95%) of respective depths overlap each other. Thereby, the only connection towards very shallow waters (10 m) is given by 20 m. Although mesophotic habitats (60 m and 80 m) are located close to each other, they do not interact. However, for 60 m only three samples were available, which results in a very flat ellipse. By considering 80 m (n = 7) as representative for the very deep mesophotic habitats instead of 60 m, the strongest positive correlation is represented by the ratio of photoprotective and light-harvesting pigments, since both are located in the same quartile (Fig. 9 A & B). Graphically more dominant than before for *Pachyseris speciosa* was *ß*-carotene [Chl a^{-1}], which featured a strong negative correlation towards mesophotic areas. On the other hand, the parameters *Symbiodinium* size, *Symbiodinium* cell density, and the lipid and protein concentrations were very strongly correlated towards each other, which is indicated by the overlapping arrows in Fig. 9 A. Since these four parameters exclusively occurred together with a great proportion of the 10 m confidence ellipse in the upper left quartile, they primarily account for very shallow habitats of *Leptoseris* spp.

In summary, deeper habitats (20 m to 80 m) showed strong interactions between each other (Fig. 9 A). These areas were mainly correlated with photoprotective pigments, rather than physiological adaptations such as *Symbiodinium* size or lipid concentration.

Table 3 Correlations and percentages of cumulative variances for *Pachyseris speciosa* (**A**: left columns) and *Leptoseris* spp. (**B**: right columns). The respective principal components (PC) with variances greater than 1 were created by principal component analysis. Explanatory variables are shown in parenthesis and significant correlations ($p < 0.05$) in bold. Tables are sorted by the respective correlations in PC 1. PP/LH represents ratio between photoprotective and light-harvesting pigments.

Variables	**PC 1**	**PC 2**	**PC 3**
PP/LH	**-0.84**	**-0.31**	**0.31**
Symbiodinium cells [10^6 cm^{-2}]	**-0.45**	**0.30**	0.05
Protein [mg cm^{-2}]	**-0.24**	0.06	**0.29**
Chlorophyll *a* [µg cm^{-2}]	**-0.21**	**0.55**	**-0.46**
(Depth [m])	0.01	**-0.24**	-0.17
Lipid [mg cm^{-2}]	0.03	-0.01	-0.12
Symbiodinium size [µm]	0.05	**0.23**	0.18
Chlorophyll *a* / Protein	0.05	**0.40**	**-0.51**
Chlorophyll c_2 Chl a^{-1}	0.07	-0.09	**0.69**
ß-carotene Chl a^{-1}	0.09	**0.82**	**-0.32**
Skeletal density [g cm^{-3}]	0.18	-0.13	-0.05
(Mitotic index)	**0.18**	0.01	-0.04
Diatoxanthin Chl a^{-1}	**0.32**	**0.79**	**0.47**
Fucoxanthin Chl a^{-1}	**0.37**	**-0.37**	**0.39**
Peridinin Chl a^{-1}	**0.76**	-0.06	0.07
Diadinoxanthin Chl a^{-1}	**0.96**	-0.19	-0.14
Xanthophyll pool Chl a^{-1}	**0.99**	-0.06	-0.06
Cumulative variance [%]	34.9	60.5	76.1

Variables	**PC 1**	**PC 2**	**PC 3**	**PC 4**	**PC 5**
Chlorophyll *a* / Protein	**-0.84**	-0.19	**0.33**	**0.24**	0.19
ß-carotene Chl a^{-1}	**-0.24**	**0.57**	0.05	0.03	**0.23**
Chlorophyll *a* [µg cm^{-2}]	-0.18	**0.49**	-0.02	-0.14	**0.62**
Xanthophyll pool Chl a^{-1}	-0.16	**0.37**	-0.05	**0.48**	**-0.23**
Skeletal density [g cm^{-3}]	-0.14	**0.38**	**-0.23**	**0.55**	-0.16
Fucoxanthin Chl a^{-1}	-0.13	**-0.26**	**0.70**	**-0.23**	0.15
Lipid [mg cm^{-2}]	0.05	**-0.25**	0.00	**-0.53**	0.14
Depth [m]	0.07	**0.65**	**-0.30**	**-0.24**	**0.31**
Protein [mg cm^{-2}]	0.16	-0.05	**-0.21**	-0.04	-0.16
Mitotic index	**0.24**	-0.04	**-0.27**	-0.13	-0.06
Diatoxanthin Chl a^{-1}	**0.28**	**-0.39**	0.15	**0.32**	**0.57**
Symbiodinium size [µm]	**0.30**	-0.15	0.03	**0.64**	-0.04
Diadinoxanthin Chl a^{-1}	**0.37**	**0.53**	**0.72**	0.02	-0.18
Peridinin Chl a^{-1}	**0.46**	**0.66**	**-0.22**	-0.06	-0.03
Symbiodinium cells [10^6 cm^{-2}]	**0.52**	0.07	0.14	**0.47**	**0.40**
PP/LH	**0.63**	**0.38**	**0.63**	-0.06	-0.19
Chlorophyll c_2 Chl a^{-1}	**0.91**	**-0.26**	-0.13	-0.09	0.04
Cumulative variance [%]	24.1	41.4	53.6	63.5	71.7

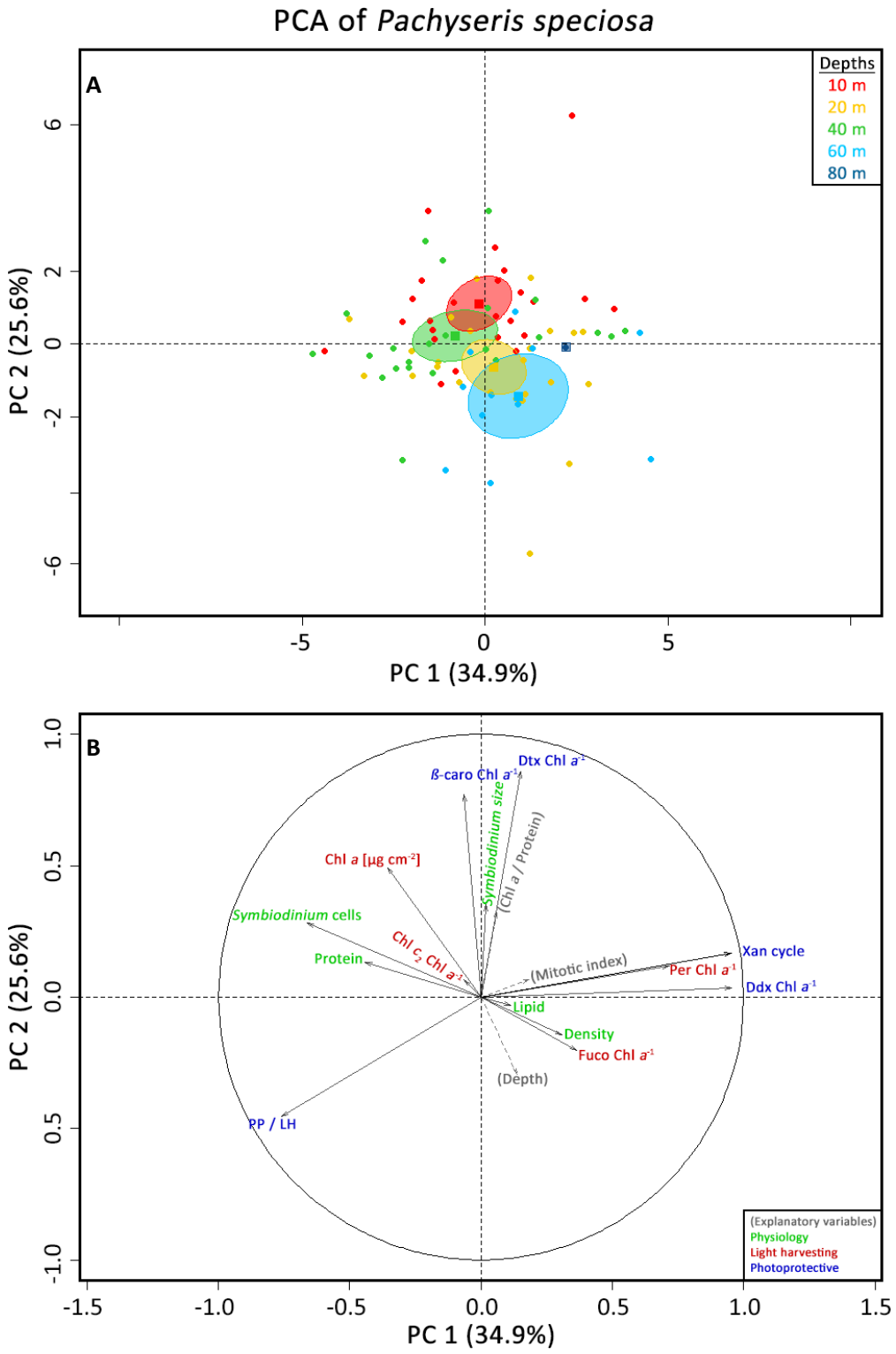

Fig. 8 Principal component analysis (PCA) of *Pachyseris speciosa* across a depth gradient 10 – 80 m. Graphs created by the first two principal components (PC) which explain in total 60.5% of the entire dataset. **(A)** Individuals graph showing *P. speciosa* at different depths. Ellipses enclose a confidence interval of 95% around the respective depth mean (square). Only one sample available at 80 m. **(B)** Variables graph showing light-harvesting (red) and photoprotective (blue) pigments, normalized to µg per area (µg cm^{-2}) and chlorophyll *a* (Chl *a*$^{-1}$) concentration, of *P. speciosa*. Explanatory variables are shown in parenthesis. Abbreviations: Chl *a* – Chlorophyll *a*, Per – Peridinin, Fuco – Fucoxanthin, Ddx – Diadinoxanthin, Dtx – Diatoxanthin, Chl c_2 – Chlorophyll c_2, ß-caro – ß-carotene, Xan cycle – xanthophyll pool per Chl *a* (Dtx + Ddx) Chl *a*$^{-1}$), PP/LH – ratio of photoprotective to light-harvesting pigments.

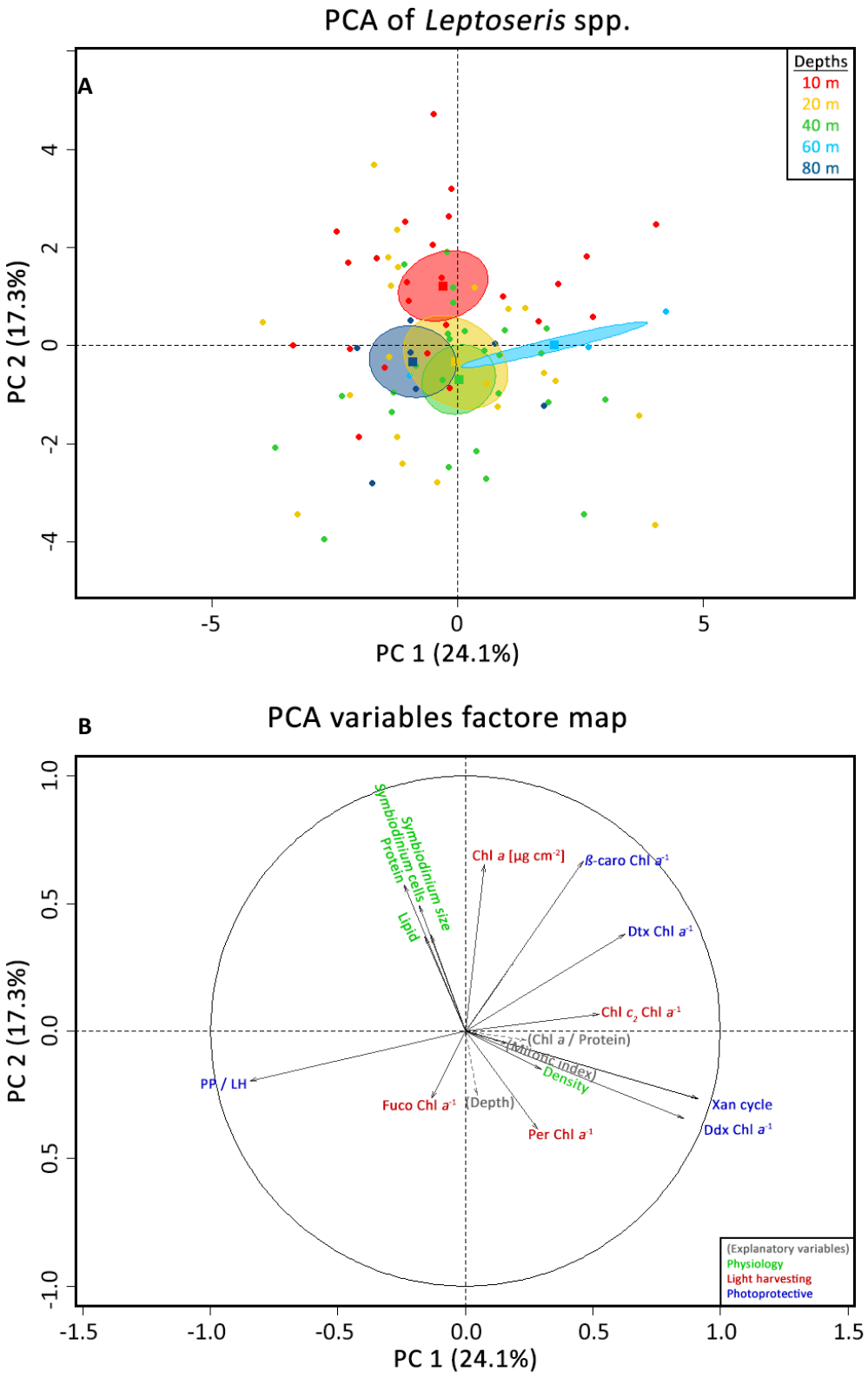

Fig. 9 Principal component analysis (PCA) of *Leptoseris* spp. (*Leptoseris scabra, Leptoseris hawaiiensis* and *Leptoseris glabra*) across a depth gradient 10 – 80 m. Graphs created by the first two principal components (PC) which explain in total 54.8% of the entire dataset. **(A)** Individuals graph showing *Leptoseris* spp. at different depths. Ellipses enclose a confidence interval of 95% around the respective depth mean (square). Only one sample available at 80 m. **(B)** Variables graph showing light-harvesting (red) and photoprotective (blue) pigments, normalized to µg per area (µg cm^{-2}) and chlorophyll *a* (Chl a^{-1}) concentration. Explanatory variables are shown in parenthesis. Abbreviations: Chl *a* – Chlorophyll *a*, Per – Peridinin, Fuco – Fucoxanthin, Ddx – Diadinoxanthin, Dtx – Diatoxanthin, Chl c_2 – Chlorophyll c_2, *ß*-caro – *ß*-carotene, Xan cycle – xanthophyll pool per Chl *a* (Dtx + Ddx) Chl a^{-1}), PP/LH – ratio of photoprotective to light-harvesting pigments.

4 Discussion

Zooxanthellate scleractinia corals exhibit physiological adaptations to cope with the reduced light-availability between shallow waters and mesophotic zones. The coral genera *Pachyseris* and *Leptoseris* feature thereby different strategies for the successful life within these habitats, which has been shown via an integrated approach of investigating the synergy of distinct photo-biological adaptations. Accordingly, the composition of light-harvesting and photoprotective pigments, physiological adjustments (skeletal density, tissue thickness and lipid concentrations), as well as *Symbiodinium* adaptations (physiology, quantities, mitotic indices) were distinguished for four different coral species: *Pachyseris speciosa* (*n* = 84), *Leptoseris scabra* (*n* = 50), *Leptoseris glabra* (*n* = 17) and *Leptoseris hawaiiensis* (*n* = 14). Since most studies in the literature only provide data on genus level (e.g. Chan *et al.*, 2009; Kahng *et al.*, 2012; Luck *et al.*, 2013; Kahng *et al.*, 2014; Pochon *et al.*, 2015; Ziegler *et al.*, 2015) a fifth group, *Leptoseris* spp. (*n* = 81), was generated by combining all *Leptoseris* samples, to allow better comparability.

4.1 Morphological adaptations promote the light-harvesting capacity in MCEs

Morphological adaptations within zooxanthellate corals have been detected across a depth gradient (10 - 80 m) in form of decreasing lipid and protein concentrations (ii).

Tropical corals can be described as lipid-rich organisms, since lipids represent a main building component of these corals (Harland *et al.*, 1992a). Lipids are used for the production of tissues, mucus and reproduction material, such as eggs or planula larvae (Stimson, 1987). Furthermore, lipid stores may be built to conserve energy (Crossland *et al.*, 1980; Stimson, 1987), which can be used for the survival of the coral colony during stress situations, as for instance in times of elevated water temperatures (Middlebrook *et al.*, 2010), shading (Harriott, 1993) or bleaching events (Yamashiro *et al.*, 2005). Field studies support the findings within this study, since also there it has been shown that different coral species feature a proportional relationship between elevated light intensities and elevated lipid concentrations (Stimson, 1987; Harland *et al.*, 1992a). Also laboratory experiments under distinct light intensities with the zooxanthellate sea anemone *Anemonia viridis* (Forskål, 1775) showed strong positive correlations between lipid concentrations and irradiance (Harland *et al.*, 1992b). In contrast, the field experiments by Harland *et al.* (1992a) showed no statistically significant decrease of the lipid concentration between 3 and 30 m for the corals *Montastrea annularis* (Ellis and Solander, 1786) and *Siderastrea siderea* (Ellis & Solander, 1768). However, *Porites porites* (Pallas, 1766) displayed statistically significant reduced lipid concentrations already at 13 m depth within this study. Furthermore, shading experiments by Harriott (1993) showed that shaded *Pocillopora damicornis* (Linnaeus, 1758) specimen utilized lipids stored as temporary energy reserve.

In contrast, *Acropora formosa* (Dana, 1846) specimen constantly increased their lipid stores, even in times of shading. This represents how different individuals of distinct coral genera maintain their lipid stores. In the framework of this study, this was also observable. While the lipid concentrations of all *Leptoseris* species showed strong correlations with the depth, the concentrations within *P. speciosa* remained relatively constant over the entire depth gradient. An explanation for the different results of the genera *Pachyseris* and *Leptoseris* might be related to differential reproduction cycles. During the process of spawning, corals utilize a lot of energy provided by lipid stores. This results in a temporary drop of the total lipid concentration, making comparisons between genera delicate (Ward, 1995; Leuzinger *et al.*, 2003; Oku *et al.*, 2003). Another reason why *P. speciosa* showed no elevated lipid concentrations at depths with higher irradiance might be its mode of nutrition. The lipid reserves of symbiotic corals may be maintained by algal photosynthesis, as well as heterotrophic feeding (Harland *et al.*, 1992a). Since *P. speciosa* seems to be a fully autotrophic organism (Veron, 2000), specimens in shallow habitats may lag the advantage of using phototrophic and heterotrophic mechanisms simultaneously to build up excessive lipid reserves in shallow areas.

Compared to the lipid concentrations, inverse results have been found for the protein concentrations per surface area. Although all species within this study showed decreasing trends over depth, only *P. speciosa* featured statistically significant results. Between 10 and 80 m water depth the protein concentration dropped by 43% for this species. For *Leptoseris* spp. it was only 25%. Significantly reduced biomass (protein concentration) of corals in habitats with low light irradiance, such as in the inside of caves (Anthony and Hoegh-Guldberg, 2003), within transplantation experiments between 5 and 20 m (Ziegler *et al.*, 2014), or across a depth gradient (10 – 60 m) (Cooper *et al.*, 2011; Ziegler *et al.*, 2015), have been found before. Thereby, specimen of *Montipora monasteriata* (Forskål, 1775), which feature a plate-like growth form similar to *Pachyseris* and *Leptoseris*, displayed 50% less surface-specific mass of protein in caves compared to specimen from open areas. And comparison between corals from open areas and specimen growing underneath overhangs delivered statistically significant results of 40% less biomass (Anthony and Hoegh-Guldberg, 2003), which confirms the findings within this study.

When combined with the chlorophyll *a* concentration, the ratio of chlorophyll *a* per unit protein [µg mg^{-1}] displayed in the literature elevated results at low light conditions (Anthony and Hoegh-Guldberg, 2003). And also studies on diatoms confirmed these findings (Chan, 1978). Likewise, this was observable in this study, though none of the species showed statistically significant ratio differences across the entire depth range.

As found within this study, decreasing protein concentrations combined with constant or decreasing amounts of *Symbiodinium* densities can typically be found in corals living in environments with low

irradiance (Iglesias-Prieto and Trench, 1997; Anthony and Hoegh-Guldberg, 2003; Ziegler *et al.*, 2015). The decrease of the *Symbiodinium* density thereby occurs especially in very dark areas and prevents self-shading to optimize the overall light-harvesting capacity of the symbiont (Fricke *et al.*, 1987; Falkowski *et al.*, 1990; Enríquez *et al.*, 2005). This is linked to a shift from *Symbiodinium* cells arranged in multiple-layers within the host tissue to *Symbiodinium* cells arranged in mono-layers at lower light conditions, which results in reduced protein concentrations (Dustan, 1979; Schlichter *et al.*, 1985, 1986; Fitt *et al.*, 2000).

Such an optimization predominantly also takes place on skeletal level. Coral colonies with smaller, more filigree and flattened growth forms are typically encountered at greater depths or in areas with reduced light levels (Anthony and Hoegh-Guldberg, 2003; Nir *et al.*, 2011; Kahng *et al.*, 2012; Englebert *et al.*, 2014). The skeletal density thereby commonly doesn't change (Anthony and Hoegh-Guldberg, 2003), as it was the case in this study. An example for changes in growth habit is represented by *M. monasteriata*. Its skeletal plate thickness within caves was 60 – 40% thinner compared to specimens from open areas (Anthony and Hoegh-Guldberg, 2003). In the framework of the present study, morphological adaptations towards reduced light environments in form of changed growth habits were however not investigable. It was not possible to distinguish the thickness of the coral fragments homogenously at a certain location of the skeleton (i.e. 2 cm from the skeletal margin) due to the small overall size of the coral fragments. Especially for coral specimen of deeper habitats, which were recovered by using an ROV, the location of the coral margin was not detectable. However, personal observations showed that coral fragments from deeper areas displayed a more filigree and thinner skeletal plate, which correlates with Anthony and Hoegh-Guldberg (2003) observations.

Within this study, it has been shown that zooxanthellate corals feature limited morphological adaptations to cope with reduced light availability in greater depths (ii). While corals of the genus *Leptoseris* predominantly featured different lipid concentrations, *Pachyseris speciosa* specimens showed strong negative correlations between protein concentrations and decreasing depth, which was probably coupled with a shift of the *Symbiodinium* arrangement from multiple-layers towards mono-layers (Dustan, 1979; Schlichter *et al.*, 1985, 1986). The different approach of the two genera might be explained by their mode of nutrition. Since *P. speciosa* exclusively retains on phototrophic feeding (Veron, 2000), more efficient morphological light-harvesting adaptations might be necessary for the survival in low light conditions (Baker *et al.*, 2015).

4.2 Adaptations of the symbiont are not primarily dictated by the depth

Adaptations related to the coral symbiont, mainly represented by changes in *Symbiodinium* size, were found across a depth range of 10 to 80 m for *Leptoseris* spp. (iii). Symbionts of *Pachyseris speciosa* displayed thereby decreasing trends of *Symbiodinium* densities.

Within the framework of this thesis, *Symbiodinium* densities and sizes, as well as mitotic indices were distinguished from *Pachyseris speciosa, Leptoseris scabra, Leptoseris glabra and Leptoseris hawaiiensis.* Statistically significant changes in *Symbiodinium* sizes across an 80 m depth gradient were exclusively found for species of the genus *Leptoseris.* Thereby, the mean size (± standard error) of healthy cells of *Leptoseris* spp. decreased from 10.3 ± 0.1 µm at shallow areas to 9.1 ± 0.2 µm at mesophotic zones. This lies in the range of other studies investigating the photo-adaptation of zooxanthellate corals across depth gradients of 10 – 40 m (Frade *et al.*, 2008a, 2008b) and 1.5 – 51 m (Wilkerson *et al.*, 1988). However, the comparison of *Symbiodinium* cell sizes between different coral species needs to be treated with caution. Depending on the genotype of the symbiont, the average *Symbiodinium* cell diameter changes since it is genetically constrained (Frade *et al.*, 2008a; Ziegler *et al.*, 2015). In example for *Madracis pharensis* (Heller, 1868) specimens from Curaçao (Caribbean) a change by up to 2 µm have been observed (Frade *et al.*, 2008a). Furthermore, it is possible that a single coral hosts multiple, co-occurring endosymbiotic strains (Iglesias-Prieto and Trench, 1997; Coffroth and Santos, 2005). Thereby, some symbiont clades feature photo-acclimatizations towards certain light regimes, which may lead to zonation; a change of symbiont types across the depth gradient within a certain coral host (Iglesias-Prieto *et al.*, 2004; LaJeunesse *et al.*, 2005; Frade *et al.*, 2007, 2008b, 2008a; Bongaerts *et al.*, 2010b). In the frame work of this Master's thesis, no genotyping of *Symbiodinium* was conducted since this project belongs to a broader study (Englebert *et al.* in prep.). Hence, the focus laid exclusively on physiological adaptation mechanisms. A phylogenetic study of the *Leptoseris* genus, as well as investigations on the *Symbiodinium* diversity of light-dependent coral species in lower mesophotic zones represent further topics of this large scale project (Englebert, PhD thesis in prep.), which will be published in combination within another format. Preliminary results indicate that all three *Leptoseris* species predominantly host symbionts of the same clade across the entire depth gradient. Though, each coral species hosted respectively different clades, which is supported by Ziegler *et al.* (2015). Furthermore, results from Bongaerts *et al.* (2011) indicate that *P. speciosa* individuals across the Great Barrier Reef harbour a single symbiont strain, belonging to clade C3, along the entire depth gradient (10 – 60 m). Across such a depth gradient, this was also observed by Cooper *et al.* (2011) at Western Australia, as well as by Ziegler *et al.* (2015) in the Red Sea. Hence, differential *Symbiodinium* clades within the coral species, but no changes across the entire depth gradient can be assumed within this thesis.

Consequently, the observed decrease in cell diameter over depth within this study is probably only indirect connected with depth, since genetic constrains limit the adaptability of certain *Symbiodinium* clades (Frade *et al.*, 2008a). For *Madracis* spp. investigations across depth gradients (5, 10, 25 and 40 m) observed, that a decrease in *Symbiodinium* size occurred only within distinct *Symbiodinium* types and started again from approximately same or elevated symbiont cell diameters as soon as a change of the symbiont type occurred. Then, the *Symbiodinium* size decreased again with increasing depth. Thereby, the symbiont change primarily occurred at 25 and 40 m depth (from B7 to B15) (Frade *et al.*, 2008a, 2008b). Accordingly, a stepwise decrease in *Symbiodinium* size was observable (Frade *et al.*, 2008a). In the framework of this study, only one sample of *Leptoseris scabra* showed at 60 m an extreme elevated cell diameter (Fig. 5 B). Symbiont genotyping revealed that this belonged to another clade than the samples from shallower depths. In the study of Frade *et al.* (2008a) the change in deeper habitats towards B15 symbionts resulted furthermore in increased protein concentrations. This was explained by the relatively larger size of B15 symbionts and the presumably higher requirement for space within the coral tissue to harbour these symbionts. It was concluded that the combination of adaptive intake of distinct *Symbiodinium* clades, the therewith coupled change in cell size, and the consequently needed space (tissue thickness), ultimately regulated the symbiont cell density. These relationships were also observable within the framework of this study. As it has been shown in the PCA for *Leptoseris* spp., the *Symbiodinium* size, *Symbiodinium* cell density, as well as the protein and lipid concentrations featured strong correlations towards each other (Fig. 9 B). On the example of the previously mentioned *L. scabra* sample from 60 m, this becomes even more obvious. Due to the relatively elevated symbiont size (Fig. 5 B) at this depth, more space within the coral tissue was needed, which can be seen at the elevated protein concentration of *L. scabra* at 60 m (Fig. 5 F). Both parameters had influence on the total *Symbiodinium* cell density, which showed a decrease at 60 m water depth (Fig. 5 A). All other symbiont cell sizes showed linear decreases over depth and therewith also linear decreases in protein concentration and symbiont density. This confirms that, except for the lower *L. scabra* specimen, overall no change of the symbiont clades across the depth gradient toke place.

As reported before (4.1), the *Symbiodinium* density of all four coral species showed a statistically non-significant decrease across a depth gradient of 80 m (Fig. 5 A). However, a downwards trend was visible, especially for *P. speciosa*. Its symbiont density almost dropped to the half from 10 m (mean ± SE) (1.09 ± 0.07 10^6 cm^{-2}) to 80 m (0.65 ± N/A 10^6 cm^{-2}), but only one sample was available for 80 m. Overall, the observed decreases are comparable to the results of other studies (Falkowski and Dubinsky, 1981; Wilkerson *et al.*, 1988; Anthony and Hoegh-Guldberg, 2003; Dove *et al.*, 2008; Frade *et al.*, 2008a; Cooper *et al.*, 2011; Ziegler *et al.*, 2015). Thereby, only the results of Cooper *et al.* (2011) and Ziegler *et al.* (2015) showed statistically significant decreases while the other authors observed

only minor decreases over depth or between irradiance levels, as present in this study. In addition to that, Fricke *et al.*, (1987) and Kaiser *et al.*, (1993) suggest that the decreasing trend of *Symbiodinium* densities might continue until corals become azooxanthellate. But with the currently deepest recorded *L. hawaiiensis* colony at 165 m (Maragos and Jokiel, 1986) and the deepest found *P. speciosa* individuals at approximately 120 m depth (Abbey *et al.*, 2013), the way towards azooxanthellate corals seems to be very long. Furthermore, the previously discussed genotype of the respective symbiont seems also to play a role (Frade *et al.*, 2008a), although, in the first place this was not observable within this study.

Same as the *Symbiodinium* densities, also the mitotic indexes displayed no statistically significant change across the depth gradient, although a minor increase of mitotic activity was noticeable between shallower and deeper habitats. These findings are supported by other investigations across a relatively large depth gradient (1.5 – 51 m) (Wilkerson *et al.*, 1988). There, highly variable mitotic indices between and within different coral species were found, ranging from 1.1% to 14.1%. Probably, differential symbiont genotypes and associated photo-adaptations were responsible for this fluctuation within coral hosts across the depth gradient (Iglesias-Prieto *et al.*, 2004).

In summary, it has been shown that the inhabiting symbionts of zooxanthellate corals feature very limited adaptations to cope with reduced light availability in greater depths (iii). Although the *Symbiodinium* size of the different *Leptoseris* species showed strong correlations with depth, this reduction probably plays only a secondary role. Other studies have found that the average size, as well as the limits of cell dimension shift, are highly correlated to the harboured *Symbiodinium* type (Iglesias-Prieto *et al.*, 2004; LaJeunesse *et al.*, 2005; Frade *et al.*, 2008a, 2008b; Ziegler *et al.*, 2015). Preliminary genotyping results of a related project showed that in average no change of the symbiont type occurred over depth, but that each of the four investigated coral species harbours distinct symbiont types. Hence, it can be concluded that the decrease in *Symbiodinium* size for *Leptoseris* spp. and the decrease of *Symbiodinium* density for *Pachyseris speciosa* are primarily driven by the hosted symbiont type, which may change over depth. Further adaptations and acclimatizations are then possible within the limitations of the respective symbiont type.

4.3 Decreasing photoprotective pigments promote the colonisation of greater depths

The composition of light-harvesting and photoprotective pigments changed across a depth gradient of 10 to 80 m within the coral genera *Pachyseris* and *Leptoseris* (iv). Thereby, especially a reduction of photoprotective pigments played a major role. In contrast, only slightly correlations with depth were observed for light-harvesting pigments.

A typical mechanism of adaptation towards reduced light levels is the increase of the light-harvesting pigment chlorophyll *a* (Falkowski and Dubinsky, 1981; Kirk, 1994; Fitt *et al.*, 2000; Dubinsky and Stambler, 2009; Kahng *et al.*, 2012), coupled with an increase of accessory pigments, such as chlorophyll c_2 , fucoxanthin or peridinin (Iglesias-Prieto and Trench, 1994; Dove *et al.*, 2006). However, this is not always the case since an excessive elevation of pigment concentrations may lead to self-shading (Fricke *et al.*, 1987; Falkowski *et al.*, 1990; Enríquez *et al.*, 2005). Hence, non-correlative relationships between chlorophyll *a* and changes in irradiance are frequently reported (Dustan, 1982; Anthony and Hoegh-Guldberg, 2003; Dove *et al.*, 2008; Cooper *et al.*, 2011; Kahng *et al.*, 2012). Dove *et al.* (2008) highlights that the correlation between chlorophyll *a* [pg cell^{-1}] and irradiance within *M. monasteriata* was significantly affected by the colour morph of the symbiont. Accordingly, especially green, red and dark brown morphs were observed in low-light habitats, while purple and tan morphs predominantly occurred in habitats with high irradiance, which consequently plays an important ecological role for the symbiont and the hosting coral (Dove *et al.*, 2006). Personal observations indicated that especially green morphs occurred within both investigated coral genera. As discussed in previous chapters (4.1 & 4.2), *Pachyseris speciosa* seems to rearrange the harboured symbionts within the coral tissue, since biomass and *Symbiodinium* density decreased over depth. Consequently, this also influenced the chlorophyll *a* concentration, which remained relatively constant across the depth gradient (both, normalized to surface area and per symbiont cell (Fig. 6 A & B)). This result is confirmed by observations of Cooper *et al.* (2011) who also found no statistically significant correlation between depth and chlorophyll *a* concentrations for *P. speciosa* across a large depth gradient (10 – 60 m) at Western Australia. In contrast, results from the Red Sea by Ziegler *et al.* (2015) showed slightly stronger correlations with water depth for *P. speciosa*. There, a gradually increase of chlorophyll *a* [fmol cell^{-1}] from 10 to 40 m was observed, which then dropped rapidly. In the framework of the present study, for all *Leptoseris* species slightly stronger correlations between chlorophyll *a* concentrations and depth were observable than for *P. speciosa*. However, also there no significances were found. Observations by Ziegler *et al.* (2015) for *Leptoseris* spp. support these findings across a 60 m gradient. Furthermore, findings of constant chlorophyll *a* concentration for *M. monasteriata* between habitats with high (open areas) and low (within caves) irradiance, further strengthen the findings that a reduction of irradiance is not always coupled with an increase in light-harvesting pigments (Anthony and Hoegh-Guldberg, 2003).

Similar results were found for other light-harvesting pigments. Chlorophyll c_2 [Chl a^{-1}] concentrations were relatively stable across the depth gradient (Fig. 6 D). Only in transition from very shallow habitats (10 m) to deeper areas a decrease was noticeable. For *P. speciosa* this was significant according to Tukey-Kramer pairwise comparisons [$F(1, 82.493) = 6.4586$, $p < 0.01$]. Such a significant decrease within the first meters, followed by relatively constant concentrations between 10 and

58 m, was also observed by Dustan (1982) for *M. annularis.* In contrast, Kaiser *et al.* (1993) found during their transplantation experiments of *Leptoseris fragilis* from 116 towards 160 m depth significant increases of chlorophyll *a* and chlorophyll c_2 concentrations. However, slow growth and reduced metabolism are common strategies for the survival in an energy-limited environment (Baker *et al.*, 2015). Hence, these adaptations might be quick responses towards the changed environment, while long-term adaptations might rather be represented by morphological adaptations, as shown within this study, or a shifts in symbiont genotype across the depth gradient (Chappell, 1980; Frade *et al.*, 2008a). Overall, the non-significant behaviour of chlorophyll c_2 [Chl a^{-1}] across large depth ranges was also observed by Ziegler *et al.* (2015) for both coral genera.

Significantly different results of peridinin [Chl a^{-1}] ratios between coral species were found by Ziegler *et al.* (2015). While concentrations remained relatively constant over depth for certain host species, it was comparably elevated in shallow habitats and then dropped for other coral species. This was also observable within the present study, where especially *Leptoseris glabra* showed significantly negative correlations with depth, while ratios within other species remained constant. Varying peridinin [µg cell^{-1}] concentrations were furthermore also present within *M. annularis* across 1 – 58 m (Dustan, 1982), as well as constant concentrations within *M. monasteriata* between open areas and within caves (Dove *et al.*, 2008). Since no changes of symbiont types across the depth gradient were observable in the studies by Ziegler *et al.* (2015), they hypothesized that the significant difference of peridinin [Chl a^{-1}] concentrations between host species, are not exclusively regulated by the respective symbiont, but rather by the hosting coral species. Hence, changes of pigment concentrations are not only regulated by the symbiont type, as suggested by (Frade *et al.*, 2008a, 2008b), which only focused on one coral genera, but also by the hosting coral species.

Overall, an increase of light-harvesting pigments across 80 m water depth was not observable, whereas significant reductions of photoprotective pigments have been found. In particular, ratios of *ß*-carotene [Chl a^{-1}] showed statistically significant negative correlations with increasing depth. Whereas the photoprotective pigment diadinoxanthin [Chl a^{-1}] and its di-epoxide partner diatoxanthin [Chl a^{-1}] showed minor significant correlations with depth, as it was also the case in the study of Ziegler *et al.* (2015). As discussed before for peridinin [Chl a^{-1}], also ratios of *ß*-carotene [Chl a^{-1}] may vary between species. While these values decrease within one species, they may remain constant or increase within other species, which has been shown quite frequently (Venn *et al.*, 2006; Frade *et al.*, 2008a, 2008b; Ziegler *et al.*, 2015). The present negative correlation between the ratio of the photoprotective *ß*-carotene [Chl a^{-1}] and depth indicate that an adaptation towards lower light levels occurred along the depth gradient.

Investigations of the xanthophyll pool [Chl a^{-1}] (sum of diadinoxanthin and diatoxanthin per chlorophyll *a*) indicated relatively constant ratios without significant correlations towards the depth gradient, although the principal component analysis (PCA) for *P. speciosa* indicated significances within the first principal component (Table 3). Typically, the xanthophyll-pool decreases with decreasing irradiance , as it has been shown for other coral species, such as *Goniastrea aspera* Verrill, 1865 or *M. monasteriata* (Brown *et al.*, 1999; Dove *et al.*, 2008; Frade *et al.*, 2008a). Thereby, the xanthophyll-pool represents a protective mechanism against elevated thermal and irradiance stress (Brown *et al.*, 1999; Venn *et al.*, 2006, 2008). However, doubts about the significance of this mechanism are raised by Venn *et al.* (2006), since no significant correlations with elevated irradiance were observed by them during bleaching experiments with corals of various genera. And also investigations between different *Symbiodinium* clades showed same results within their study. In fact, Ziegler *et al.* (2015) observed for *Pachyseris* spp. and *Leptoseris* spp. also no significant decrease of the xanthophyll de-epoxidation (xanthophyll pools [Chl a^{-1}] are not presented) across 60 m depth, while it showed different pattern for corals of the genus *Porites*. Furthermore, observations by Frade *et al.* (2008a) showed that some *Madracis* species featured decreasing xanthophyll pool [Chl a^{-1}] ratios while others showed relatively constant ratios between 5 and 40 m water depth. This demonstrate how diverse different coral genera and species respond with photoprotective mechanisms towards decreasing light levels and supports the here observed data.

In summary, most of the photoprotective and light-harvesting (PP/LH) pigments displayed no significant change between 10 and 80 m water depth (iv). Predominantly decreases of photoprotective pigments, such as *ß*-carotene [Chl a^{-1}] or diadinoxanthin [Chl a^{-1}], across the depth gradient represented adaptations towards declining light levels, rather than increases of light-harvesting pigments. However, these adaptations occurred only in a limited extend, as shown by the non-significant PP/LH ratio and xanthophyll pool [Chl a^{-1}] and are probably constrained and regulated by the symbiont type and the hosting coral species (Frade *et al.*, 2008a; Ziegler *et al.*, 2015).

4.4 Interacting adaptations are the key for a successful conisation of a depth gradient

This study revealed, that multiple interactions of physiological parameters, rather than some highly significant changes, are present within the coral genera *Pachyseris* and *Leptoseris*, to cope with decreasing light levels. Thereby, *Pachyseris* and *Leptoseris* featured significantly different strategies. A principal component analyses showed that *Pachyseris speciosa* is more correlated to the protein concentration, *Symbiodinium* density, as well as chlorophyll c_2 [Chl a^{-1}] and *ß*-carotene [pg cell^{-1}] concentrations. In contrast, species of the genus *Leptoseris* altogether rather accounted for strongly decreasing lipid concentrations and smaller *Symbiodinium* sizes (i). Respectively, these parameters

also represented main adaptation mechanisms to optimize the light-harvesting capability in greater depths.

In shallow waters (10 m), an elevated chlorophyll c_2 [Chl a^{-1}] ratio combined with high *Symbiodinium* densities played a significant role for *P. speciosa* to enhance the light-harvesting capacity. This was linked to high concentrations of the photoprotective pigments diatoxanthin and *ß*-carotene, which presumably acted as photoprotective light filter in times of highly increased irradiance (Choudhury and Behera, 2001; Schagerl and Müller, 2006; Dubinsky and Stambler, 2009). In comparison to species of the genus *Leptoseris,* the chlorophyll c_2 [Chl a^{-1}] and *ß*-carotene [Chl a^{-1}] ratios were significantly higher across the entire depth range. In contrast, species of the genus *Leptoseris* showed in shallow habitats significantly elevated light-harvesting pigment ratios of peridinin [Chl a^{-1}] and chlorophyll *a* [Chl a^{-1}], coupled with comparably lower photoprotective pigment concentrations. This probably facilitated the build-up of significantly elevated lipid stores, compared to *P. speciosa* (Crossland *et al.*, 1980; Stimson, 1987; Harland *et al.*, 1992a; Harriott, 1993). This demonstrates that the genera *Pachyseris* and *Leptoseris* already in shallow waters feature minor differences in light-harvesting mechanisms, which influence furthermore the morphology of the hosting coral (Harland *et al.*, 1992b).

When comparing the strategies in deeper areas, these findings become even more obvious (Ziegler *et al.*, 2015). *P. speciosa* showed a statistically significant decrease in protein [mg cm^{-2}] concentration, combined with a strong negative trend of the *Symbiodinium* density [10^6 cm^{-2}] across 10 – 80 m, which was also reported by Cooper *et al.* (2011) and Ziegler *et al.* (2015) for *P. speciosa*. This suggests that a rearrangement of the *Symbiodinium* cells from multiple-layers towards an mono-layer arrangement occurred to reduce self-shading of the symbionts (Dustan, 1979; Schlichter *et al.*, 1985, 1986; Fricke *et al.*, 1987; Falkowski *et al.*, 1990; Fitt *et al.*, 2000). Consequently, tissue thickness (protein concentration) decreased, which furthermore promoted the light-harvesting capacity of the hosting coral. This optimization was coupled with a significant decrease of the photoprotective pigment *ß*-carotene [Chl a^{-1}], which furthermore promoted the light-harvesting capacity in low-light environments (Jeffrey and Haxo, 1968; Falkowski and Dubinsky, 1981; Kirk, 1994; Brown *et al.*, 1999; Dubinsky and Stambler, 2009; Kahng *et al.*, 2012). These adaptations thereby occurred and interacted across the entire depth range and are not restricted to certain depth, as it has been shown by a PCA (Fig. 8 A).

In contrast to *P. speciosa*, all *Leptoseris* species showed relatively same results towards each other (ANOVA analyses and PCA (Fig. 4)). Same as for *P. speciosa*, photoprotective concentrations, such as *ß*-carotene and diatoxanthin concentrations, dropped with increasing depth. This was combined with a significant decrease in *Symbiodinium* cell size, which is a common strategy in low light environments

to reduce self-shading (Wilkerson *et al.*, 1988; Frade *et al.*, 2008a, 2008b). However, this variation in symbiont cell size is genetically constrained and therefore maybe a shift towards better adapted symbiont genotypes occurs in greater depths (Iglesias-Prieto *et al.*, 2004; LaJeunesse *et al.*, 2005; Frade *et al.*, 2007, 2008b, 2008a; Bongaerts *et al.*, 2010b). As consequence of the decreasing light availability and only relatively minor adaptations, the excessive lipid stores rapidly vanished. This demonstrates that corals of the genus *Leptoseris* are highly tolerant organisms which thrive very well in a broad range of different environments (Veron, 2000).

In summary (v), the coral host had a strong effect on the photo-adaptation strategy (i), as it was also found by (Ziegler *et al.*, 2015). While *Pachyseris speciosa* showed stronger morphological adaptations in form of decreasing protein concentrations (ii) and *Symbiodinium* densities (iii), corals of the genus *Leptoseris* rather decreased their symbiont size (iii). However, both had in common that they decreased their photoprotective pigment concentrations, rather than increasing their light-harvesting pigments (iv).

Besides all this, endolithic algae, which can be harboured within the coral skeleton, may also play a certain role in the adaptability towards lower light levels. A few specimen of each coral species hosted endolithic algae at 20 m within this study. Furthermore, one *Leptoseris scabra* sample from 80 m depth featured endolithic algae within its skeleton. It has been shown that endolithic algae are highly adapted towards harsh environments and that their photo-assimilates may be used by the hosting coral colony (Shashar *et al.*, 1997). This, predominantly occurs during bleaching events and by promoting the survival of the coral during this stress situation (Fine and Loya, 2002). Within mesophotic corals, endolithic algae were also reported as great source of energy, even exceeding the beneficial relationship within corals from shallower habitats (Schlichter *et al.*, 1997; Kahng *et al.*, 2012). However, still very little is known about endolithic algae and their role for the colonisation of mesophotic reefs.

5 Conclusions and outlook

Overall it can be concluded, that multiple interactions of physiological parameters, rather than some highly significant changes, seem to be the key for a successful colonisation of a large depth range, as it has been shown for the coral genera *Pachyseris* and *Leptoseris* (v). Thereby, *Leptoseris* seems to be a relatively less specific depth-generalist than *Pachyseris* (i), which is able to conquer various habitats with only minor adaptations (decreasing symbiont size (iii) and decreasing concentrations of photoprotective pigments (iv)) due to its relatively higher tolerance towards environmental conditions (Veron, 2000; Ziegler *et al.*, 2015). This can be seen on the excessive lipid reserves stored in shallower habitats, as well as only few statistically significant changes across the depth gradient. In contrast, *Pachyseris speciosa* seems to be relatively more specific, since it not only showed adaptations in form of reduced photoprotective pigments (iv), but also by a presumable rearrangements of the symbionts (iii), coupled with decreases of the tissue thickness and *Symbiodinium* densities (ii).

However, further investigations regarding changes in symbiont genotype across the depth gradient (Frade *et al.*, 2008a), influences of varying symbiont colour morphs (Dove *et al.*, 2008), effects of harboured endolithic algae (Schlichter *et al.*, 1997; Kahng *et al.*, 2012), as well as micro-skeletal changes (Kahng *et al.*, 2012) need to be conducted in future. Furthermore, studies across greater depths need to be performed, since 80 m depth are just the beginning of the lower mesophotic zone and healthy *Leptoseris* and *Pachyseris* colonies have been found down to 120 m and beyond (Maragos and Jokiel, 1986; Abbey *et al.*, 2013). Therewith, it will be possible to bring light into the darkness of mesophotic zones, by unravelling their key for the successful colonisation of very large depth ranges.

6 Acknowledgements

I would like to express my appreciation to the XL Catlin Seaview Survey and the Global Change Institute of the University of Queensland who funded this research project. In addition, I would like to thank the German Academic Exchange Service (DAAD) for a stipend to cover my travel costs between Germany and Australia.

My greatest appreciation and gratitude goes to Dr. Pim Bongaerts and Norbert Englebert for the project development and the very nice working environment both of you created. My gratitude extents to the entire staff of the Coral Reef Ecosystems Laboratory of the University of Queensland, in particular Associate Professor Sophie Dove and Dr. Annamieke Van den Heuvel. It was a pleasure and a great honour to work with all of you in this laboratory.

Furthermore, I am grateful for the very friendly and flexible support by Professor Kai Bischof. Without his help, this thesis would not have been possible.

In addition, I would like to thank Dr. Kyra Hay and the crew of the Mike Ball for their great support during the process of sampling. Likewise, Dr. Zena Dinesen and Dr. Paul Muir provided invaluable assistance during taxonomic determinations. A special thanks goes to Christiane Hassenrück, who greatly helped in the process of data analysis. In addition, I would like to express my gratitude to Professor Christian Wild, Ramona Brunner and Don Song for their helpful suggestions as reviewers of this manuscript.

Finally, I would like to express my deepest gratitude to my family. Without their support, all this would not have been possible. Thank you so much for your love.

I dedicate this thesis to my grandparents who passed away during my time abroad. I wish that they could see me graduate and move on to another stage in my life…

7 References

Abbey, E., Webster, J.M., Braga, J.C., Jacobsen, G.E., Thorogood, G., Thomas, A.L., Camoin, G., Reimer, P.J., Potts, D.C., 2013. Deglacial mesophotic reef demise on the Great Barrier Reef. Palaeogeography, Palaeoclimatology, Palaeoecology 392, 473–494.

Adams, A.J., Dahlgren, C.P., Kellison, Gt., Kendall, M.S., Layman, C.A., Ley, J.A., Nagelkerken, I., Serafy, J.E., 2006. Nursery function of tropical back-reef systems. Marine Ecology Progress Series 318, 287–301.

Anthony, K.R.N., Hoegh-Guldberg, O., 2003. Variation in coral photosynthesis, respiration and growth characteristics in contrasting light microhabitats: an analogue to plants in forest gaps and understoreys? Functional Ecology 17, 246–259.

Armstrong, R.A., Singh, H., Torres, J., Nemeth, R.S., Can, A., Roman, C., Eustice, R., Riggs, L., Garcia-Moliner, G., 2006. Characterizing the deep insular shelf coral reef habitat of the Hind Bank marine conservation district (US Virgin Islands) using the Seabed autonomous underwater vehicle. Continental Shelf Research 26, 194–205.

Baker, A.C., Glynn, P.W., Riegl, B., 2008. Climate change and coral reef bleaching: An ecological assessment of long-term impacts, recovery trends and future outlook. Estuarine, Coastal and Shelf Science 80, 435–471.

Baker, E.K., Puglise, K.A., Harris, P.T., (in review) (Eds.), 2015. Mesophotic reefs – A life boat for coral reefs? The United Nations Environment Programme and GRID-Arendal, Nairobi and Arendal.

Bongaerts, P., Frade, P.R., Hay, K.B., Englebert, N., Latijnhouwers, K.R.W., Bak, R.P.M., Vermeij, M.J.A., Hoegh-Guldberg, O., 2015. Deep down on a Caribbean reef: Lower mesophotic depths harbor a specialized coral-endosymbiont community. Scientific Reports 5, 7652.

Bongaerts, P., Ridgway, T., Sampayo, E.M., Hoegh-Guldberg, O., 2010a. Assessing the “deep reef refugia” hypothesis: focus on Caribbean reefs. Coral Reefs 29, 309–327.

Bongaerts, P., Riginos, C., Ridgway, T., Sampayo, E.M., van Oppen, M.J., Englebert, N., Vermeulen, F., Hoegh-Guldberg, O., 2010b. Genetic divergence across habitats in the widespread coral *Seriatopora hystrix* and its associated *Symbiodinium*. PLoS one 5, e10871.

Bongaerts, P., Sampayo, E., Bridge, T., Ridgway, T., Vermeulen, F., Englebert, N., Webster, J., Hoegh-Guldberg, O., 2011. *Symbiodinium* diversity in mesophotic coral communities on the Great Barrier Reef: a first assessment. Marine Ecology Progress Series 439, 117–126.

Brown, B.E., 1990. Damage and recovery of coral reefs affected by El Niño related seawater warming in the Thousand Islands, Indonesia. Coral reefs 8, 163–170.

Brown, B.E., Ambarsari, I., Warner, M.E., Fitt, W.K., Dunne, R.P., Gibb, S.W., Cummings, D.G., 1999. Diurnal changes in photochemical efficiency and xanthophyll concentrations in shallow water reef corals: evidence for photoinhibition and photoprotection. Coral Reefs 18, 99–105.

Brown, B.E., Zamani, N.P., 1993. Mitotic indices of zooxanthellae: a comparison of techniques based on nuclear and cell division frequencies. Marine Ecology-Progress Series 89, 99–99.

Chan, A.T., 1978. Comparative physiological study of marine diatoms and dinoflagellates in relation to irradiance and cell size. I. Growth under continuous light. Journal of Phycology 14, 396–402.

Chan, Y.L., Pochon, X., Fisher, M.A., Wagner, D., Concepcion, G.T., Kahng, S.E., Toonen, R.J., Gates, R.D., 2009. Generalist dinoflagellate endosymbionts and host genotype diversity detected from mesophotic (67-100 m depths) coral *Leptoseris*. BMC Ecology 9, 21.

Chappell, J., 1980. Coral morphology, diversity and reef growth. Nature 286, 249–252.

Choudhury, N.K., Behera, R.K., 2001. Photoinhibition of photosynthesis: role of carotenoids in photoprotection of chloroplast constituents. Photosynthetica 39, 481–488.

Coffroth, M.A., Santos, S.R., 2005. Genetic diversity of symbiotic dinoflagellates in the genus *Symbiodinium*. Protist 156, 19–34.

Connell, J.H., 1978. Diversity in tropical rain forests and coral reefs. Science 199, 1302–1310.

Cooper, T.F., Ulstrup, K.E., Dandan, S.S., Heyward, A.J., Kuhl, M., Muirhead, A., O’Leary, R.A., Ziersen, B., van Oppen, M.J.H., 2011. Niche specialisation of reef-building corals in the mesophotic zone: metabolic trade-offs between divergent *Symbiodinium* types. Proc R Soc B 278, 1840 – 1855.

Crossland, C.J., Barnes, D.J., Borowitzka, M.A., 1980. Diurnal lipid and mucus production in the staghorn coral *Acropora acuminata*. Marine Biology 60, 81–90.

Davies, P.S., 1989. Short-term growth measurements of corals using an accurate buoyant weighing technique. Mar Biol 101, 389–395.

Dinesen, Z.D., 1980. A revision of the coral genus *Leptoseris* (Scleractinia: Fungiina: Agariciidae). Memoirs of the Queensland Museum 20, 181–235.

Dove, S.G., Lovell, C., Fine, M., Deckenback, J., Hoegh-Guldberg, O., Iglesias-Prieto, R., Anthony, K.R.N., 2008. Host pigments: potential facilitators of photosynthesis in coral symbioses. Plant, Cell & Environment 31, 1523–1533.

Dove, S., Ortiz, J.C., Enriquez, S., Fine, M., Fisher, P., Iglesias-Prieto, R., Thornhill, D., Hoegh-Guldberg, O., 2006. Response of holosymbiont pigments from the scleractinian coral *Montipora monasteriata* to short-term heat stress. Limnology and Oceanography 51, 1149–1158.

Dubinsky, Z., Stambler, N., 2009. Photoacclimation processes in phytoplankton: mechanisms, consequences, and applications. Aquatic Microbial Ecology 56, 163–176.

Dunnett, C.W., 1980. Pairwise multiple comparisons in the homogeneous variance, unequal sample size case. Journal of the American Statistical Association 75, 789–795.

Dunn, S.R., Thomas, M.C., Nette, G.W., Dove, S.G., 2012. A lipidomic approach to understanding free fatty acid lipogenesis derived from dissolved inorganic carbon within Cnidarian-Dinoflagellate symbiosis. PLoS ONE 7, e46801.

Dustan, P., 1982. Depth-dependent photoadaptation by zooxanthellae of the reef coral *Montastrea annularis*. Marine Biology 68, 253–264.

Dustan, P., 1979. Distribution of zooxanthellae and photosynthetic chloroplast pigments of the reef-building coral *Montastrea annularis* Ellis and Solander in relation to depth on a west Indian coral reef. Bulletin of Marine Science 29, 79–95.

Englebert, N., Bongaerts, P., Muir, P., Hay, K.B., Hoegh-Guldberg, O., 2014. Deepest zooxanthellate corals of the Great Barrier Reef and Coral Sea. Marine Biodiversity.

Enríquez, S., Méndez, E.R., Iglesias-Prieto, R., 2005. Multiple scattering on coral skeletons enhances light absorption by symbiotic algae. Limnology and Oceanography 50, 1025–1032.

Falkowski, P.G., Dubinsky, Z., 1981. Light-shade adaptation of *Stylophora pistillata*, a hermatypic coral from the Gulf of Eilat. Nature 289, 172–174.

Falkowski, P.G., Jokiel, P.L., Kinzie, R.A., 1990. Irradiance and corals, in: Ecosystems of the World. Elsevier, Amsterdam, pp. 89–107.

Feingold, J.S., 2001. Responses of three coral communities to the 1997–98 El Niño–Southern Oscillation: Galapagos Islands, Ecuador. Bulletin of marine science 69, 61–77.

Fine, M., Loya, Y., 2002. Endolithic algae: an alternative source of photoassimilates during coral bleaching. Proceedings of the Royal Society of London B: Biological Sciences 269, 1205–1210.

Fitt, W.K., McFarland, F.K., Warner, M.E., Chilcoat, G.C., 2000. Seasonal patterns of tissue biomass and densities of symbiotic dinoflagellates in reef corals and relation to coral bleaching. Limnology and oceanography 45, 677–685.

Folch, J., Lees, M., Sloane-Stanley, G., 1956. A simple method for the isolation and purification of total lipids from animal tissues. J. biol. Chem 226, 497–509.

Frade, P.R., Bongaerts, P., Winkelhagen, A.J.S., Tonk, L., Bak, R.P.M., 2008a. *In situ* photobiology of corals over large depth ranges: A multivariate analysis on the roles of environment, host, and algal symbiont. Limnology and Oceanography 53, 2711.

Frade, P.R., De Jongh, F., Vermeulen, F., Van Bleijswijk, J., Bak, R.P.M., 2007. Variation in symbiont distribution between closely related coral species over large depth ranges. Molecular Ecology 17, 691–703.

Frade, P.R., Englebert, N., Faria, J., Visser, P.M., Bak, R.P.M., 2008b. Distribution and photobiology of *Symbiodinium* types in different light environments for three colour morphs of the coral *Madracis pharensis*: is there more to it than total irradiance? Coral Reefs 27, 913–925.

Fricke, H.W., Vareschi, E., Schlichter, D., 1987. Photoecology of the coral *Leptoseris fragilis* in the Red Sea twilight zone (an experimental study by submersible). Oecologia 73, 371–381.

Glynn, P.W., 1996. Coral reef bleaching: facts, hypotheses and implications. Global Change Biology 2, 495–509.

Glynn, P.W., Maté, J.L., Baker, A.C., Calderón, M.O., 2001. Coral bleaching and mortality in Panama and Ecuador during the 1997–1998 El Niño–Southern Oscillation event: spatial/temporal patterns and comparisons with the 1982–1983 event. Bulletin of Marine Science 69, 79–109.

Graham, N.A., Wilson, S.K., Jennings, S., Polunin, N.A.J., Robinson, J., Bijoux, J.P., Daw, T.M., 2007. Lag effects in the impacts of mass coral bleaching on coral reef fish, fisheries, and ecosystems. Conservation Biology 21, 1291–1300.

Harland, A.D., Davies, P.S., Fixter, L.M., 1992a. Lipid content of some Caribbean corals in relation to depth and light. Marine Biology 113, 357–361.

Harland, A.D., Fixter, L.M., Davies, P.S., Anderson, R.A., 1992b. Effect of light on the total lipid content and storage lipids of the symbiotic sea anemone *Anemonia viridis*. Marine Biology 112, 253–258.

Harriott, V.J., 1993. Coral lipids and environmental stress. Environmental monitoring and assessment 25, 131–139.

Hinderstein, L.M., Marr, J.C.A., Martinez, F.A., Dowgiallo, M.J., Puglise, K.A., Pyle, R.L., Zawada, D.G., Appeldoorn, R., 2010. Theme section on "Mesophotic coral ecosystems: characterization, ecology, and management." Coral Reefs 29, 247–251.

Hoaglin, D.C., Iglewicz, B., 1987. Fine-tuning some resistant rules for outlier labeling. Journal of the American Statistical Association 82, 1147–1149.

Hoegh-Guldberg, O., 1999. Climate change, coral bleaching and the future of the world's coral reefs. Marine and freshwater research 50, 839–866.

Hoegh-Guldberg, O., 1988. A method for determining the surface area of corals. Coral Reefs 7, 113–116.

Hoegh-Guldberg, O., Mumby, P.J., Hooten, A.J., Steneck, R.S., Greenfield, P., Gomez, E., Harvell, C.D., Sale, P.F., Edwards, A.J., Caldeira, K., 2007. Coral reefs under rapid climate change and ocean acidification. Science 318, 1737–1742.

Hoffmeister, T.S., Babendreier, D., Wajnberg, E., 2006. *13* Statistical tools to improve the quality of experiments and data analysis for assessing non-target effects. Environmental Impact of Invertebrates for Biological Control of Arthropods: Methods and Risk Assessment 1, 1–222.

Holstein, D.M., 2013. Vertical connectivity in mesophotic coral ecosystems. University of Miami.

Hsu, J.C., 1996. Multiple Comparisons: Theory and Methods.

Hughes, T.P., Baird, A.H., Bellwood, D.R., Card, M., Connolly, S.R., Folke, C., Grosberg, R., Hoegh-Guldberg, O., Jackson, J.B.C., Kleypas, J., 2003. Climate change, human impacts, and the resilience of coral reefs. Science 301, 929–933.

Hughes, T.P., Tanner, J.E., 2000. Recruitment failure, life histories, and long-term decline of Caribbean corals. Ecology 81, 2250–2263.

Humphrey, G.F., Jeffrey, S.W., 1997. Tests of accuracy of spectrophotometric equations for the simultaneous determination of chlorophylls *a, b, c1* and *c2*. Phytoplankton Pigments in Oceanography: Guidelines to Modern Methods. Monographs on Oceanographic Methodology 616–621.

Iglesias-Prieto, R., Beltran, V.H., LaJeunesse, T.C., Reyes-Bonilla, H., Thome, P.E., 2004. Different algal symbionts explain the vertical distribution of dominant reef corals in the eastern Pacific. Proceedings of the Royal Society of London, Series B: Biological Sciences 271, 1757–1763.

Iglesias-Prieto, R., Trench, R.K., 1997. Acclimation and adaptation to irradiance in symbiotic dinoflagellates. II. Response of chlorophyll–protein complexes to different photon-flux densities. Marine Biology 130, 23–33.

Iglesias-Prieto, R., Trench, R.K., 1994. Acclimation and adaptation to irradiance in symbiotic dinoflagellates. I. Responses of the photosynthetic unit to changes in photon flux density. Marine ecology progress series. Oldendorf 113, 163–175.

Jantzen, C., Laudien, J., Sokol, S., Försterra, G., Häussermann, V., Kupprat, F., Richter, C., 2013. *In situ* short-term growth rates of a cold-water coral. Mar Freshw Res 64, 631–641.

Jeffrey, S.W., Haxo, F.T., 1968. Photosynthetic pigments of symbiotic dinoflagellates (zooxanthellae) from corals and clams. The Biological Bulletin 135, 149–165.

Johannes, R.E., Wiebe, W.J., 1970. Method for determination of coral tissue biomass and composition. Limnology and Oceanography 15, 822–824. doi:10.4319/lo.1970.15.5.0822

Jokiel, P.L., Maragos, J.E., Franzisket, L., 1978. Coral growth: buoyant weight technique, in: Coral Reefs: Research Methods. UNESCO, Paris, pp. 379–396.

Kahng, S., Copus, J., Wagner, D., 2014. Recent advances in the ecology of mesophotic coral ecosystems (MCEs). Current Opinion in Environmental Sustainability 7, 72–81.

Kahng, S.E., 2013. Growth rate for a zooxanthellate coral (*Leptoseris hawaiiensis*) at 90m. Galaxea, Journal of Coral Reef Studies 15, 39–40.

Kahng, S.E., Garcia-Sais, J.R., Spalding, H.L., Brokovich, E., Wagner, D., Weil, E., Hinderstein, L., Toonen, R.J., 2010. Community ecology of mesophotic coral reef ecosystems. Coral Reefs 29, 255–275.

Kahng, S., Hochberg, E., Apprill, A., Wagner, D., Luck, D., Perez, D., Bidigare, R., 2012. Efficient light harvesting in deep-water zooxanthellate corals. Marine Ecology Progress Series 455, 65–77.

Kaiser, P., Schlichter, D., Fricke, H.W., 1993. Influence of light on algal symbionts of the deep water coral *Leptoseris fragilis*. Marine Biology 117, 45–52.

Keppel, G., Wickens, T.D., 2004. Design and analysis: A researcher's handbook.

Kirk, J.T.O., 1994. Light and photosynthesis in aquatic ecosystems. Cambridge University Press, Cambridge.

Kühlmann, D.H.H., 1983. Composition and ecology of deep-water coral associations. Helgoländer Meeresuntersuchungen 36, 183–204.

Küster, F.W., Thiel, A., Fischbeck, K., 1972. Logarithmische Rechentafeln, 101st ed. Walter de Gruyter, Berlin.

LaJeunesse, T.C., Lambert, G., Andersen, R.A., Coffroth, M.A., Galbraith, D.W., 2005. *Symbiodinium* (Pyrrhophyta) genome sizes (DNA content) are smallest among dinoflagellates. Journal of Phycology 41, 880–886.

Latasa, M., Van Lenning, K., Garrido, J.L., Scharek, R., Estrada, M., Rodríguez, F., Zapata, M., 2001. Losses of chlorophylls and carotenoids in aqueous acetone and methanol extracts prepared for RPHPLC analysis of pigments. Chromatographia 53, 385–391.

Lê, S., Josse, J., Husson, F., 2008. FactoMineR: An R package for multivariate analysis. Journal of statistical software 25, 1–18.

Leuzinger, S., Anthony, K.R.N., Willis, B.L., 2003. Reproductive energy investment in corals: scaling with module size. Oecologia 136, 524–531.

Lewis, D.G., 1971. The analysis of variance, 1st ed. Manchester University Press, Manchester.

Liddell, W.D., Ohlhorst, S.L., 1988. Hard substrata community patterns, 1-120 m, North Jamaica. Palaios 3, 413–423.

Luck, D.G., Forsman, Z.H., Toonen, R.J., Leicht, S.J., Kahng, S.E., 2013. Polyphyly and hidden species among Hawai'i's dominant mesophotic coral genera, *Leptoseris* and *Pavona* (Scleractinia: Agariciidae). PeerJ 1, e132.

Maragos, J.E., Jokiel, P.L., 1986. Reef corals of Johnston Atoll: one of the world's most isolated reefs. Coral Reefs 4, 141–150.

Mardia, K.V., 1970. Measures of multivariate skewness and kurtosis with applications. Biometrika 57, 519–530.

Marsh, J.A., 1970. Primary productivity of reef-building calcareous red algae. Ecology 51, 255–263.

Martin, W.E., Bridgmon, K.D., 2012. Quantitative and statistical research methods: From hypothesis to results. John Wiley & Sons, San Francisco.

Meyer, J.L., Schultz, E.T., 1985. Tissue condition and growth rate of corals associated with schooling fish. Limnology and Oceanography 30, 157–166.

Middlebrook, R., Anthony, K.R.N., Hoegh-Guldberg, O., Dove, S., 2010. Heating rate and symbiont productivity are key factors determining thermal stress in the reef-building coral *Acropora formosa*. Journal of Experimental Biology 213, 1026–1034.

Milliken, G.A., Johnson, D.E., 2009. Analysis of messy data volume 1: designed experiments, 2nd ed. CRC Press, Boca Raton, Florida.

Moberg, F., Folke, C., 1999. Ecological goods and services of coral reef ecosystems. Ecological Economics 29, 215–233.

Müller, P., Li, X.-P., Niyogi, K.K., 2001. Non-photochemical quenching. A response to excess light energy. Plant physiology 125, 1558–1566.

Nagelkerken, I., van der Velde, G., Gorissen, M.W., Meijer, G.J., Van't Hof, T., Hartog, C. den, 2000. Importance of mangroves, seagrass beds and the shallow coral reef as a nursery for important coral reef fishes, using a visual census technique. Estuarine, Coastal and Shelf Science 51, 31–44.

Nir, O., Gruber, D.F., Einbinder, S., Kark, S., Tchernov, D., 2011. Changes in scleractinian coral *Seriatopora hystrix* morphology and its endocellular *Symbiodinium* characteristics along a bathymetric gradient from shallow to mesophotic reef. Coral Reefs 30, 1089–1100.

Nir, O., Gruber, D.F., Shemesh, E., Glasser, E., Tchernov, D., 2014. Seasonal mesophotic coral bleaching of *Stylophora pistillata* in the Northern Red Sea.

Oku, H., Yamashiro, H., Onaga, K., Sakai, K., Iwasaki, H., 2003. Seasonal changes in the content and composition of lipids in the coral *Goniastrea aspera*. Coral Reefs 22, 83–85.

Palumbi, S.R., Barshis, D.J., Traylor-Knowles, N., Bay, R.A., 2014. Mechanisms of reef coral resistance to future climate change. Science 344, 895–898.

Pochon, X., Forsman, Z.H., Spalding, H.L., Padilla-Gamino, J.L., Smith, C.M., Gates, R.D., 2015. Depth specialization in mesophotic corals (*Leptoseris* spp.) and associated algal symbionts in Hawai'i. Royal Society Open Science 2, 140351–140351.

Porra, R.J., 2005. The chequered history of the development and use of simultaneous equations for the accurate determination of chlorophylls *a* and *b*, in: Discoveries in Photosynthesis. Springer, pp. 633–640.

Porra, R.J., Thompson, W.A., Kriedemann, P.E., 1989. Determination of accurate extinction coefficients and simultaneous equations for assaying chlorophylls *a* and *b* extracted with four different solvents: verification of the concentration of chlorophyll standards by atomic absorption spectroscopy. Biochimica et Biophysica Acta (BBA)-Bioenergetics 975, 384–394.

Porter, J.W., Muscatine, L., Dubinsky, Z., Falkowski, P.G., 1984. Primary production and photoadaptation in light-and shade-adapted colonies of the symbiotic coral, *Stylophora pistillata*. Proceedings of the Royal Society of London B: Biological Sciences 222, 161–180.

Pratchett, M.S., Munday, P., Wilson, S.K., Graham, N.A., Cinner, J.E., Bellwood, D.R., Jones, G.P., Polunin, N.V., McClanahan, T.R., 2008. Effects of climate-induced coral bleaching on coral-reef fishes. Ecological and economic consequences. Oceanography and Marine Biology: Annual Review 46, 251–296.

Razali, N.M., Wah, Y.B., 2011. Power comparisons of Shapiro-Wilk, Kolmogorov-Smirnov, Lilliefors and Anderson-Darling tests. Journal of Statistical Modeling and Analytics Vol 2, 21–33.

R Core Team, 2015. *R*: A language and environment for statistical computing. R Foundation for Statistical Computing, Vienna, Austria.

Riegl, B., Piller, W.E., 2003. Possible refugia for reefs in times of environmental stress. International Journal of Earth Sciences 92, 520–531.

Schagerl, M., Müller, B., 2006. Acclimation of chlorophyll *a* and carotenoid levels to different irradiances in four freshwater cyanobacteria. Journal of plant physiology 163, 709–716.

Schlichter, D., Fricke, H.W., Weber, W., 1986. Light harvesting by wavelength transformation in a symbiotic coral of the Red Sea twilight zone. Marine Biology 91, 403–407.

Schlichter, D., Kampmann, H., Conrady, S., 1997. Trophic potential and photoecology of endolithic algae living within coral skeletons. Marine Ecology 18, 299–317.

Schlichter, D., Weber, W., Fricke, H.W., 1985. A chromatophore system in the hermatypic, deep-water coral *Leptoseris fragilis* (Anthozoa: Hexacorallia). Marine Biology 89, 143–147.

Shapiro, S.S., Wilk, M.B., 1965. An analysis of variance test for normality (complete samples). Biometrika 52, 591–611.

Shashar, N., Banaszak, A.T., Lesser, M.P., Amrami, D., 1997. Coral endolithic algae: life in a protected environment. Pacific Science 51, 167–173.

Shaw, R.G., Mitchell-Olds, T., 1993. Anova for unbalanced data: an overview. Ecology 74, 1638–1645.

Slattery, M., Lesser, M.P., Brazeau, D., Stokes, M.D., Leichter, J.J., 2011. Connectivity and stability of mesophotic coral reefs. Journal of Experimental Marine Biology and Ecology 408, 32–41.

Spencer, T., 1985. Marine erosion rates and coastal morphology of reef limestones on Grand Cayman Island, West Indies. Coral Reefs 4, 59–70.

Stimson, J., Kinzie III, R.A., 1991. The temporal pattern and rate of release of zooxanthellae from the reef coral *Pocillopora damicornis* (Linnaeus) under nitrogen-enrichment and control conditions. Journal of Experimental Marine Biology and Ecology 153, 63–74.

Stimson, J.S., 1987. Location, quantity and rate of change in quantity of lipids in tissue of Hawaiian hermatypic corals. Bulletin of Marine Science 41, 889–904.

Strychar, K.B., 2002. Bleaching in soft and scleractinian corals: comparison of the physiology, genetics, and biochemistry of *Symbiodinium* (PhD Thesis). Faculty of Arts, Health and Sciences, Central Queensland University.

Strychar, K.B., Coates, M., Sammarco, P.W., Piva, T.J., Scott, P.T., 2005. Loss of *Symbiodinium* from bleached soft corals *Sarcophyton ehrenbergi*, *Sinularia* sp. and *Xenia* sp. Journal of experimental marine biology and ecology 320, 159–177.

Sunamura, T., 1992. Geomorphology of rocky coasts. John Wiley & Sons Ltd, Chichester.

Takabayashi, M., Hoegh-Guldberg, O., 1995. Ecological and physiological differences between two colour morphs of the coral *Pocillopora damicornis*. Marine Biology 123, 705–714.

Tukey, J.W., 1977. Exploratory data analysis. Addison Wesley.

van Oppen, M.J.H., Bongaerts, P., Underwood, J.N., Peplow, L.M., Cooper, T.F., 2011. The role of deep reefs in shallow reef recovery: an assessment of vertical connectivity in a brooding coral from west and east Australia: vertical connectivity in a brooding coral. Molecular Ecology 20, 1647–1660.

Vareschi, E., Fricke, H., 1986. Light responses of a scleractinian coral (*Plerogyra sinuosa*). Marine Biology 90, 395–402.

Veal, C.J., Carmi, M., Fine, M., Hoegh-Guldberg, O., 2010. Increasing the accuracy of surface area estimation using single wax dipping of coral fragments. Coral Reefs 29, 893–897.

Venn, A.A., Loram, J.E., Douglas, A.E., 2008. Photosynthetic symbioses in animals. Journal of Experimental Botany 59, 1069–1080.

Venn, A.A., Weber, F.K., Loram, J.E., Jones, R.J., 2009. Deep zooxanthellate corals at the high latitude Bermuda Seamount. Coral reefs 28, 135–135.

Venn, A.A., Wilson, M.A., Trapido-Rosenthal, H.G., Keely, B.J., Douglas, A.E., 2006. The impact of coral bleaching on the pigment profile of the symbiotic alga, *Symbiodinium*. Plant, Cell & Environment 29, 2133–2142.

Veron, J.E.N., 2000. Corals of the World, vol. 3. Australian Institute of Marine Science & CRR Qld Pty Ltd, Australia.

Veron, J.E.N., 1986. Corals of Australia and the Indo-Pacific. Angus & Robertson, London.

Ward, S., 1995. The effect of damage on the growth, reproduction and storage of lipids in the scleractinian coral *Pocillopora damicornis* (Linnaeus). Journal of Experimental Marine Biology and Ecology 187, 193–206.

Wellington, G.M., Glynn, P.W., Strong, A.E., Navarrete, S.A., Wieters, E., Hubbard, D., 2001. Crisis on coral reefs linked to climate change. Eos, Transactions American Geophysical Union 82, 1–5.

West, J.M., Salm, R.V., 2003. Resistance and resilience to coral bleaching: implications for coral reef conservation and management. Conservation Biology 17, 956–967.

Whitaker, J.R., Granum, P.E., 1980. An absolute method for protein determination based on difference in absorbance at 235 and 280 nm. Analytical biochemistry 109, 156–159.

Whitlock, M.C., Schluter, D., 2009. The analysis of biological data. Roberts and Company Publishers, Greenwood Village, Colorado.

Wilkerson, F.P., Kobayashi, D., Muscatine, L., 1988. Mitotic index and size of symbiotic algae in Caribbean reef corals. Coral reefs 7, 29–36.

Yamashiro, H., Oku, H., Onaga, K., 2005. Effect of bleaching on lipid content and composition of Okinawan corals. Fisheries Science 71, 448–453.

Zapata, M., Rodriguez, F., Garrido, J.L., 2000. Separation of chlorophylls and carotenoids from marine phytoplankton: a new HPLC method using a reversed phase C8 column and pyridine-containing mobile phases. Marine Ecology Progress Series 195, 29–45.

Ziegler, M., Roder, C.M., Büchel, C., Voolstra, C.R., 2015. Mesophotic coral depth acclimatization is a function of host-specific symbiont physiology. Frontiers in Marine Science 2, 10.

Ziegler, M., Roder, C.M., Büchel, C., Voolstra, C.R., 2014. Limits to physiological plasticity of the coral *Pocillopora verrucosa* from the central Red Sea. Coral Reefs 33, 1115–1129.

8 Declaration of authorship

Hereby I declare that I have written this Master's Thesis by my own and without any assistance from third parties. Furthermore, I confirm that no other sources and resources have been used than those indicated in the thesis itself and that all quotations are marked.

_____
Christopher Andreas Nowak

Date of submission: 14 September 2015